Iranian Journal of Chemistry and Chemical Engineering (IJCCE)

Experimental studies on use of nanofluid and glass cover cooling on the performance of hemispherical solar still: Energy and Exergy Approach

"Mohammed El Hadi Attia [1], Murshitha Shajahan[2], Muthu Manokar[3*], Ahmed Kadhim Hussein[4], Elimame Elaloui[5], Hussein Togun[6], Lioua Kolsi[7,8]

[1] Physics Department, Faculty of Exact Sciences, University of El Oued, 3900, El Oued, Algeria, attiameh@gmail.com

[2]Department of Electronics and Instrumentation Engineering, B.S. Abdur Rahman Crescent Institute of Science and Technology, Chennai 600048, Tamil Nadu, India. murshitha@crescent.education

[*3]Department of Mechanical Engineering, B.S. Abdur Rahman Crescent Institute of Science and Technology, Ch8ennai 600048, Tamil Nadu, India, a.muthumanokar@gmail.com

[4] Mechanical Engineering Department, College of Engineering, University of Babylon - Babylon City - Hilla - Iraq, E-mail addresses: ahmedkadhim7474@gmail.com

[5]Laboratory of the application of materials to the environment, water, and energy (LR21ES15), Faculty of Sciences of Gafsa, Gafsa University, Tunisia. limam.aloui@fsgf.u-gafsa.tn

[6] Biomedical Engineering Department, University of Thi-Qar, 64001 Nassiriya, Iraq

Email: htokan_2004@yahoo.com; hussein-tokan@utq.edu.iq

[7] Department of Mechanical Engineering, College of Engineering, University of Ha'il, Ha'il City 2440, Saudi Arabia (E-mail: lioua_enim@yahoo.fr)

[8] Laboratory of Metrology and Energy Systems, Department of Energy Engineering, University of Monastir, Monastir 5000, Tunisia"

*Email: a.muthumanokar@gmail.com

Abstract

The impact of using TiO_2 nano-coated basin and glass cover cooling at different concentrations of 0.1, 0.2, and 0.3% on Traditional Hemispherical Solar Still (THSS) was researched at El Oued City, Algeria. From the research output, it is found that by adding nano-coated basin at concentrations of 0.1, 0.2, and 0.3% in the HSS, the output distilled water of 4.07, 4.54, and 4.96 kg was obtained. The use of nano-coated basin at concentrations of 0.1, 0.2, and 0.3% with glass cooling in the HSS produced the output distilled water of 4.9, 5.47, and 6.12 kg, respectively. Furthermore, energy and exergy efficiencies are calculated. The diurnal energy efficiency obtained for the HSS with a nano-coated basin at concentrations of 0.1, 0.2, and 0.3% is found as 33.24, 37.61, and 41%, while the daily exergy efficiency is 2.52, 3.03, and 3.47%, respectively. Similarly, the daily energy efficiency obtained for the HSS with a nano-coated basin at concentrations of 0.1, 0.2, and 0.3% with glass cooling are found to be 40.34, 46 and 51%, while the daily exergy efficiency is 3.32, 4.07, and 4.71%, respectively.

Keywords: Hemispherical solar still; distillation; Nano-coating; forced condensation; cover cooling; exergy analysis

1. Introduction

Water is important for all living things, including living beings, plants, animals, and people. One of the most serious difficulties that human civilization has faced, particularly in third-world countries, is choosing who can provide safe, clean water at a reasonable cost **[1-2].** Desalination of water has emerged as a scientifically and economically practical solution to the problems connected with increasing water scarcity in many parts of the world **[3-4].** In the last ten years, solar distillation systems have received a lot of interest from scientists and academics to convert sea or brackish water into high-purity freshwater utilizing clean and free solar energy **[5-6].** Distillation requires the use of solar energy to heat salt water that can be supplied from solar power or any other low-cost source. Solar energy is a highly efficient energy source, a clean energy and alternative to fossil fuels, and is good for the environment for a range of applications such as water heating, and distillation **[7-10].** The working principle is relatively basic, and it is quite similar to the well-known evaporation-condensation cycle that occurs in nature, such as when rain falls. Survey papers on solar distillation have been referred to [11-18].

Researchers are trying to find new ways to improve SS performance, such as cumulative distillate yield, expanding surface area, adding energy storage materials, and inventing unique designs **[19-24].** All of these variables, according to their findings, have a considerable impact on SS productivity, particularly during the spring and winter seasons. **Ismail [25]** employed a hemispherical SS to improve the quantity of solar energy captured by the SS and decrease the shadow of the SS walls. The efficiency and productivity of a hemispherical design are linearly related to the depth of the water. Despite the enormous number of articles published on various SS styles, the number of works on HSS is now very limited. Under the climate circumstances in Coimbatore (India), **Arunkumar et al. [26]** reported the performance of the hemispherical top cover SS where the water flowing to cool the still cover was examined in the first case. In another case, the flow was not taken into consideration. It was concluded that, by cooling the cover of the HSS, the efficiency was enhanced from 34% to 42%. **Raju et al. [27]** explored the prospect of increasing the efficiency of an HSS by combining it with evacuated tubes, a parabolic reflector concentrator, and heat pipes in Bangalore City's outdoor settings (India). On the other hand, **Hijleh Abu [28] and Hijleh Abu & Mousa [29]** investigated the performance of HSS by using a water layer over a single glass HSS. They used the "film cooling parameters," which resulted in a 20% improvement in SS efficiency when used for evaporation from the film, compared to just 6% when not utilized for evaporation. **Mohd Zaheen et al. [30]** have numerically evaluated the influence of top cover cooling on the performance of HSS. Water flow over the SS reduces cover temperature, enhancing the system's daily yield and resulting in a 34 to 42% increase in HSS efficiency.

The addition of nanoparticles is one of the techniques to increase the SS's output. **Sahota and Tiwari [31]** used Al_2O_3 and **Sahota and Tiwari [32]** used TiO_2. in a double slope SS: The use of nanofluids in double slope SS enhanced the accumulated distillate generated hourly and daily, according to their findings. **Madhu et al. [33]** used Al_2O_3, TiO_2, and CuO as nanofluids in the stepped SS. **Kabeel et al. [34]** investigated a basin-type SS with a black-painted Cu_2O_4 nanoparticle absorber plate. **Kabeel et al. [35]** investigated the external heat exchanger and the use of Al_2O_3 nanofluids on solar distillation yield. The addition of an external heat exchanger enhances the output by 53.2%. The combined effect of the condenser and Al_2O_3 nanofluids in SS enhances the output by 116%. In an experimental context, **Kabeel et al. [36]** examine the impact of a fan and the addition of 0.2 percent Al_2O_3 nanofluids on the yield of a SS. The combined effect of the operating fan and nanofluids enhances productivity by 125 percent. **Shanmugan et al. [37]** examined the performance of a SS using Al_2O_3. **Subhedar [38]** examined the influence of Al_2O_3 nanoparticles in a SS at varying volume concentrations. The researchers discovered that a volume concentration of 0.1 percent Al_2O_3 nanoparticles increases productivity when compared to 0.05 percent Al_2O_3 nanoparticles.

Kabeel et al. [39] published the impact of water depth on a pyramid SS coated with TiO_2 nano black paint. They employed a new SS with a basin coated with TiO_2 nanoparticles mixed with black paint to increase the SS output. The results found that the distilled yield was improved by about 6.1% by using TiO_2 nano black paint. **Shanmugan et al. [40]** investigated experimentally a SS with a TiO_2 nano bed for natural freshwater innovation under a variety of operating conditions, including coating the basin liner with TiO_2 nanoparticles mixed with Cr_2O_3 and various hybrid bond adsorption combinations. The daily yield of the SS was 7.89 and 5.39 L during the summer and winter, respectively. Shayanmehr & Mahdavi investigated the CSS using spraying water and a fog condenser [41]. Norouzi & Bozorgian [42] utilized the waste exhaust gas in the desalination plant. The CSS generated a daily yield of 4.4 kg using a black cotton wick [43]. Bahrami et al. 2019 used CSS with a dish concentrator to obtain a yield of 75 kg per day [44]. Fallahzadeh et al. investigated the novel portable active still [45].

Parikh et al. [46] employed TiO_2 and a black die mixture as a base paint to determine the performance of the SS at 20 and 40% weight by weight in a combination of TiO_2 materials and a black die mixture. They discovered that a 20 percent and 40 percent mixture increased productivity by 11–18 percent and 20–23 percent, respectively, as related to conventional SS. Nanoparticles were used in PCM for improving heat energy storage capacity [47-53] and few researchers used nanoparticle coatings in SS basins [54-56].

Novelty statement:

A review of recent advances and development of HSS was referred to [6]. From the review [6] it is found that only a few manuscripts were reported on the use of nano-particles and glass cooling. The freshwater yield from HSS using nano-TiO_2 has not been investigated yet, as evidenced by the above-mentioned works of literature. As a result, the objective of this paper is to investigate improving the productivity of HSS using different concentrations of nano-TiO_2 and constant flow cover cooling technique.

2. Titanium oxide nano‐particles preparation method

Sol-Gel is the most process used to synthesize TiO_2 pure or doped nanoparticles **[57 - 61]**. The Strober method or a modified sol-gel route known permit to obtain TiO_2 mesoporous nanoparticles using a surfactant agent.

2.1 Synthesis of TiO_2 nanoparticles in the presence of structuring agents

The synthesis of mesoporous titanium nanoparticles was carried out using a modified sol-gel technique with the use of structuring agents. The process described in **Figure 1** illustrates the different steps taken during the synthesis. In the first step, the surfactant is solubilized in water to generate the formation of spherical micelles, then with the addition of hydrolyzed titanium precursor, there will be self-assembly of this precursor around the micelles formed to obtain titanium nanoparticles. The last step and the elimination of surfactant to form pores inside an inorganic matrix.

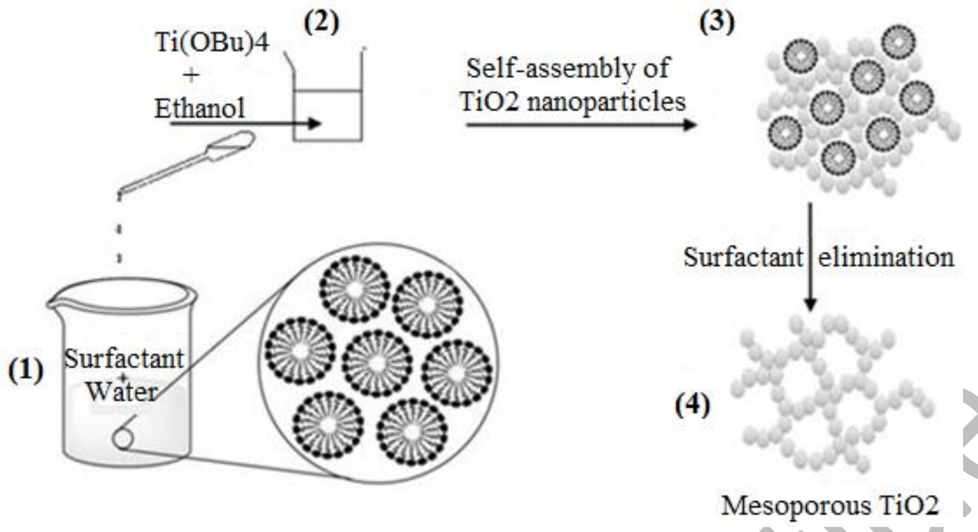

Fig.1. Schematic illustration of the formation of mesoporous titanium oxide spheres.

The synthesis protocol is as follows: Typically, 200 mg of surfactant and 60 mL of distilled water were mixed under agitation until complete dissolution. Then, a solution containing 1 mL of $Ti(OBu)_4$ precursor and 20 mL of ethanol was added drop by drop to the first solution, stirring strongly at 40°C. Thus, the milky white solution formed has been kept in agitation for 12 h and then collected by centrifugation for 15 min. Subsequently, the elimination of the surfactant was carried out by the extraction method using an alcoholic solution of ammonium nitrate NH_4NO_3 (6 g/L) then wash three times with water and ethanol. Finally, the air-dried product is recovered.

2.2 Characterization of TiO_2 nanoparticles

Using a Hitachi S- 2600N, Transmission Electron Microscopy (TEM) images were produced (employing a detector made of secondary electrons). The particles were mixed in ethanol before being put onto copper grids covered in porous carbon sheets for TEM examination. Using a Micromeritics Autochem ASAP 2020 V3.00H machine, measurements of nitrogen adsorption-desorption at 77 K were made to determine the specific surface area and pore structure parameters of the materials. Measurements of X-ray diffraction (XRD) were made using a PANalytical X'Pert MPD (Philips 1710). The Cu Ka radiation was used to gather the XRD patterns.

2.2.1 TEM

TEM images are shown in **Figure 2**. They reveal the presence of a large quantity of very small particles with an average size of about 50 nm while constituting a disordered network which is a typical feature of mesoporous structures.

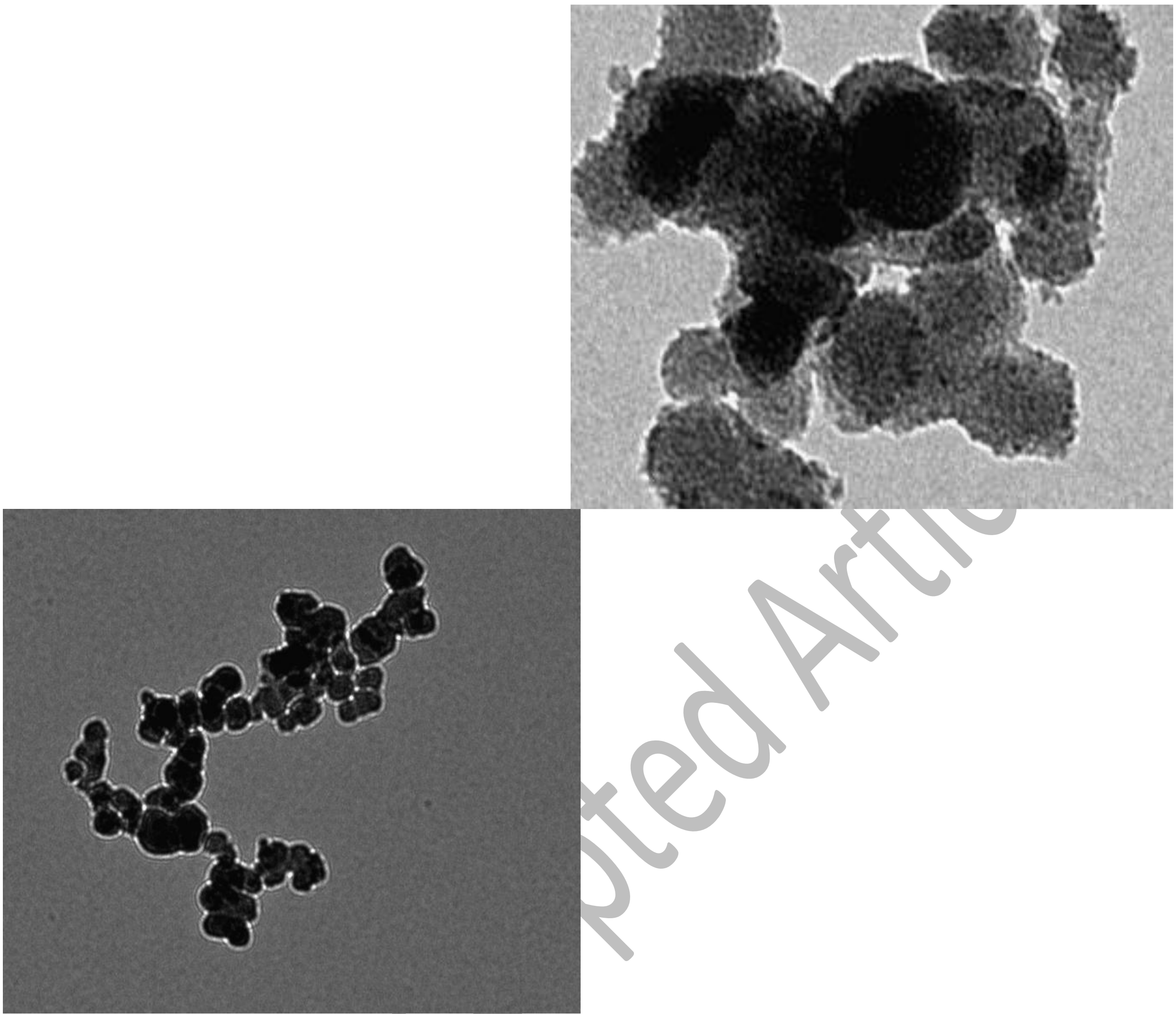

Samples at 200 nm Samples at 50 nm

Fig. 2. TEM images of TiO_2 samples at 200 nm and 50 nm

2.2.2. Desorption/ adsorption of liquid N2 at 77 K

Figure 3 illustrates the adsorption/desorption isotherms of liquid nitrogen at 77 K of the synthesized sample. The isotherm obtained is a Type IV characteristic of mesoporous materials according to the IUPAC classification. In addition, the increase in adsorption is rapid at pressures below 0.4 which implies that the particles have wide pores. This can also be confirmed by the observation of hysteresis type H1, characteristic of mesopore, which is because the desorption of the nitrogen condensed by capillarity in the pores is not reversible.

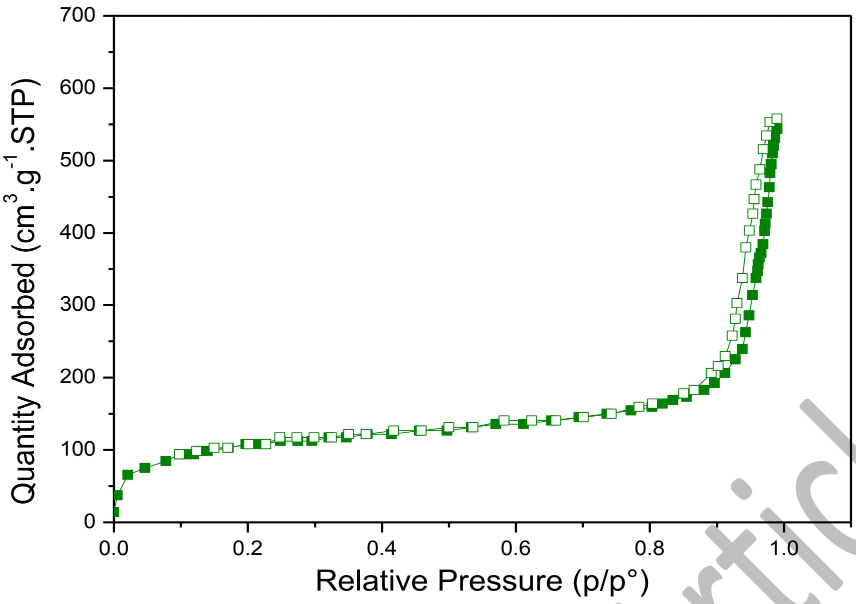

Fig.3. The adsorption/desorption isotherms of liquid nitrogen at 77 K of TiO_2 nanoparticle

The specific surfaces obtained by the BET method, as well as the pore size distribution (pore diameter and volumes) obtained by the BJH method (Barett-Joyner-Halenda) are presented in **Table 1**.

Table 1: The specific surfaces obtained by the BET method.

Sample	**SBET ($m^2.g^{-1}$)**	**D pores (nm)**	**V pores ($cm^3.g^{-1}$)**
TiO_2 Nanoparticle	437	8.54	1.01

2.2.3 XRD

The X-ray diffraction of the sample is shown in **Figure 4.** It shows that all peaks have been well-defined and can be observed. In addition, the phase mainly formed for all prepared materials is anatase. The peaks located at 2θ = {25,3; 37,8; 48,1; 54,0} correspond to the reticular planes (101), (004), (200), (105), and (211) according to the JCPDS files (Joint Committee of Powder Diffraction Standards, Map No: 21-1272).

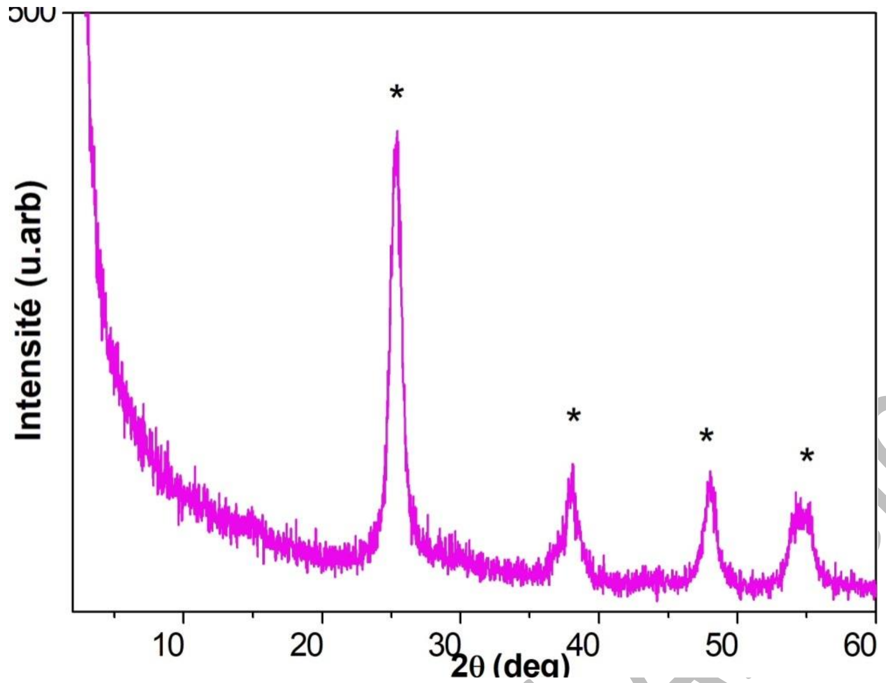

Fig. 4. TiO_2 nanoparticle diffractogram

3. Experimental setup

The performance of the HSS using TiO_2 nanoparticles at varying concentrations with constant flow cover cooling was experimented. Three hemispherical basins made of wood with a 50 mm thickness, each with a surface area of 0.1 m^2. Each basin was 40 mm in depth and 380 mm in diameter. To better capture solar radiation, the interior surfaces of the HSS have been coated with black silicon. The HSS was 400 mm in diameter and was covered with a 3 mm thick plastic cap hemispherical cover as indicated in **Figure 5**. **Figure 6** represents a picture of the experimental setup. The three HSS were experimented on for three days in the same climate of El Oued city Algerian. The TiO_2 nanoparticles' specifications are listed in **Table 2**. Three experiments were carried out in this research using three different TiO_2 concentrations. The first experiment compares three distillers: HSS, HSS with 0.1% of nano TiO_2 coated basin, and HSS with 0.1% of nano TiO_2 coated basin with cover cooling a constant flow at 2.5 L/h. The second experiment compares three distillers: HSS, HSS with 0.2% of nano TiO_2 coated basin, and HSS with 0.2% of nano TiO_2 coated basin with cover cooling a constant flow at 2.5 L/h. The Third experiment compares three distillers: HSS, HSS with 0.3% of nano TiO_2 coated basin, and HSS with 0.3% of nano TiO_2 coated basin with cover cooling a constant flow at 2.5 L/h.

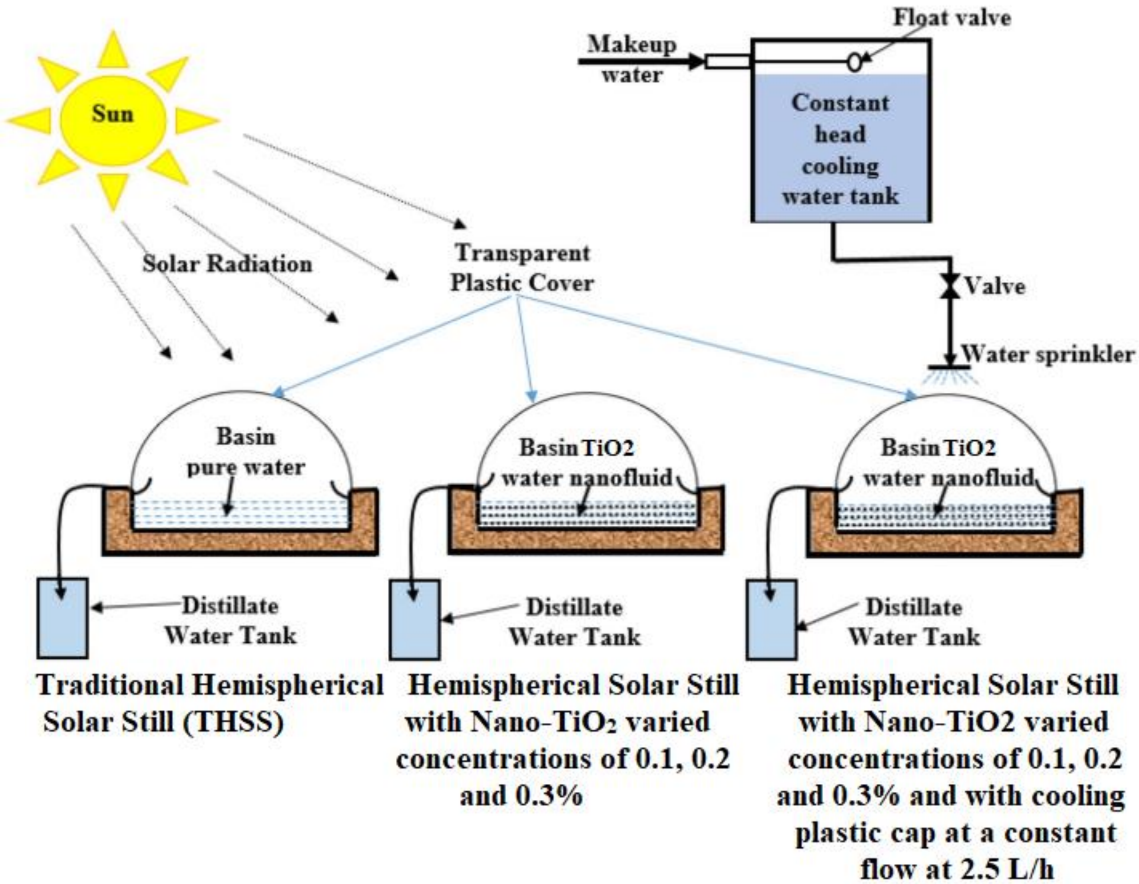

Fig. 5. Experimental trial rig schematic diagram.

Table 2: The TiO_2 nanoparticles' specifications

Specifications	Units	TiO_2 Nanoparticles
Thermal conductivity	[W/(m.K)]	8.4
Density	[g/cm^3]	4.23
Specific heat, C_p	[J/kg.K]	692
Melting Point	[˚C]	1843
Boiling Point	[˚C]	2972
Average particles size	[nm]	50
Appearance		White powder

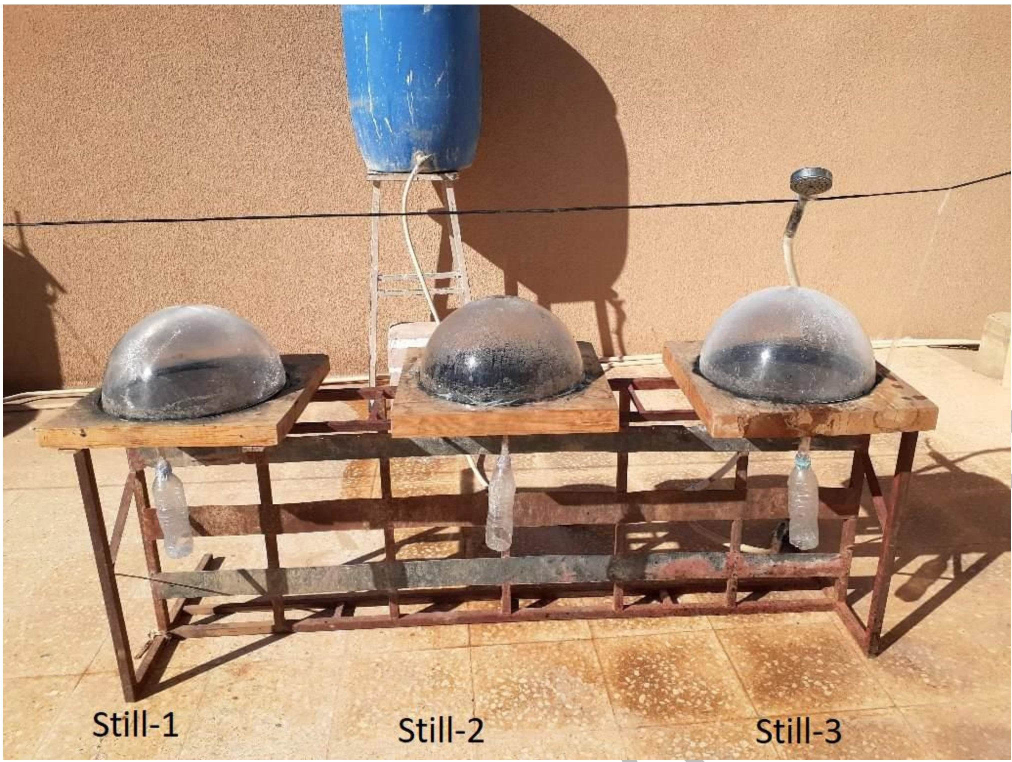

Fig. 6. Photograph of tests setup.

The experiments were conducted in three various situations, as displayed in **Table 3**.

Table 3: Types of experiments conducted.

Experiment	SS 1	SS 2	SS 3
Day-1	THSS	HSS with 0.1% of nano TiO_2 coated basin	HSS with 0.1% of nano TiO_2 coated basin with cover cooling
Day-2	THSS	HSS with 0.2% of nano TiO_2 coated basin	HSS with 0.2% of nano TiO_2 coated basin with cover cooling
Day-3	THSS	HSS with 0.3% of nano TiO_2 coated basin	HSS with 0.3% of nano TiO_2 coated basin with cover cooling

The examinations tested for 10 hours, with a saltwater depth of 1.0 cm in all HSS. **Table 4** records measurement instruments, as well as their accuracy and standard errors.

Table 4: Instruments, accuracy, and standard uncertainties.

Instrument	Accuracy	Range	Standard uncertainty
Solar power meter	± 10 W/m^2	0-1999 W/m^2	5.77 W/m^2
Thermocouple	± 0.1 ˚C	−100–500 ˚C	0.06 ˚C
Graduated cylinder	± 1 mL	0–250 mL	0.6 mL

4. Results and discussions

4.1 performance of THSS, HSS with 0.1% of nano TiO_2 coated basin, and HSS with 0.1% of nano TiO_2 coated basin with cover cooling

The impact of using nanomaterial with different concentrations in HSS is being investigated. The real-time experiments were performed for three different days for various concentrations of nano-TiO_2 with constant flow cover cooling to improve the output of HSS. Figure 7 represents the intermittent variation of solar radiation (It), ambient temperature (T_a), Water Temperature (T_w), and glass Temperature (T_g) on day-1. The solar radiation reached its maximum around noon on all three days. The average solar radiation of day-1 is 682.90 W/m^2. The average T_a of day-1 was 32.3˚C. Which is comparatively high and it means the sunny conditions of the day. The difference between T_w and T_g in the THSS, HSS with 0.1% of nano TiO_2 coated basin, and HSS with 0.1% of nano TiO_2 coated basin with cover cooling is in the range of 3 to 10˚C, 5 to 11˚C and 6 to 12˚C, separately. Since the temperature difference between T_w and T_g of HSS with 0.1% of nano TiO_2 coated basin with cover cooling is more, the yield was higher in this case as compared to other cases. The average T_w of THSS, HSS with 0.1% of nano TiO_2 coated basin, and HSS with 0.1% of nano TiO_2 coated basin with cover cooling are 48.9˚C, 50.9˚C, and 49.8˚C, separately. The average T_g of THSS, HSS with 0.1% of nano TiO_2 coated basin, and HSS with 0.1% of nano TiO_2 coated basin with cover cooling is 43.3˚C, 44.10˚C, and 41.4˚C, respectively. The average temperature variation between T_w and T_g of THSS, HSS with 0.1% of nano TiO_2 coated basin, and HSS with 0.1% of nano TiO_2 coated basin with cover cooling is 5.6, 6.8, and 8.4°C, respectively. it's inferred that the average T_w and T_g of HSS with 0.1% of nano TiO_2 coated basin with cover cooling is 49.80˚C and 41.40˚C which is 1.1 ˚C and 2.7 ˚C lower than the average T_w and T_g of HSS with of nano TiO_2 coated basin. The drop in temperature is due to the cooling effect of the HSS cover with 0.1% of nano TiO_2 coated basin with cover cooling. According to the comparison tests, utilizing nano TiO_2 improves the HSS's performance. The surface area of the HSS with 0.1% of nano TiO_2 coated basin, and HSS with 0.1% of nano TiO_2 coated basin with cover cooling is higher than that of the THSS. Therefore, HSS with TiO_2 nanoparticles has a higher Tw than the Tw of the THSS.

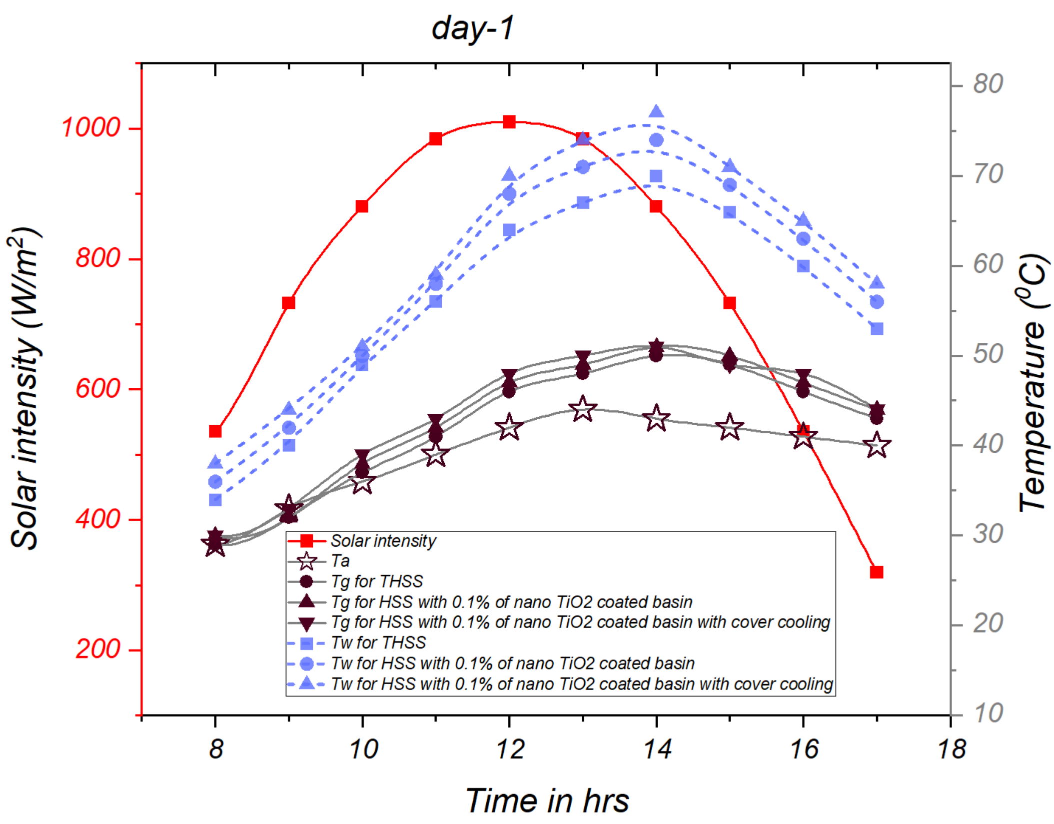

Fig. 7. Variations of It, T_a, T_w, T_g of SS on day-1

Figure 8 shows the variations of the Evaporative Heat Transfer Coefficient (EHTC) and productivity of THSS, HSS with 0.1% of nano TiO_2 coated basin, and HSS with 0.1% of nano TiO_2 coated basin with cover cooling. The maximum EHTC of THSS, HSS with 0.1% of nano TiO_2 coated basin, and HSS with 0.1% of nano TiO_2 coated basin with cover cooling are 36.94, 43.35, and 48.61 W/m^2K, respectively. The maximum hourly productivity of THSS, HSS with 0.1% of nano TiO_2 coated basin, and HSS with 0.1% of nano TiO_2 coated basin with cover cooling are 0.87, 1.05, and 0.98 kg, separately. The daily yield of THSS, HSS with 0.1% of nano TiO_2 coated basin, and HSS with 0.1% of nano TiO_2 coated basin with cover cooling are 3.70, 4.79, and 5.48 kg, individually. The diurnal average EHTC of HSS with 0.1% of nano TiO_2 coated basin and HSS with 0.1% of nano TiO_2 coated basin with cover cooling is 30.18 and 29.21 W/m^2K, respectively which is higher than the THSS. The maximum hourly yield produced by the HSS with 0.1% of nano Tio_2 coated basin is 1.05 kg. Higher EHTC is found from the graph due to the high temperature in HSS with 0.1% of nano TiO_2 coated basin compared with THSS. Higher EHTC tends to maximize yield. The nano TiO_2 on the HSS increases Tw, EHTC, and yield compared to the THSS because the nano-coated absorber plate enhances the thermal conductivity and surface area of the absorber plate.

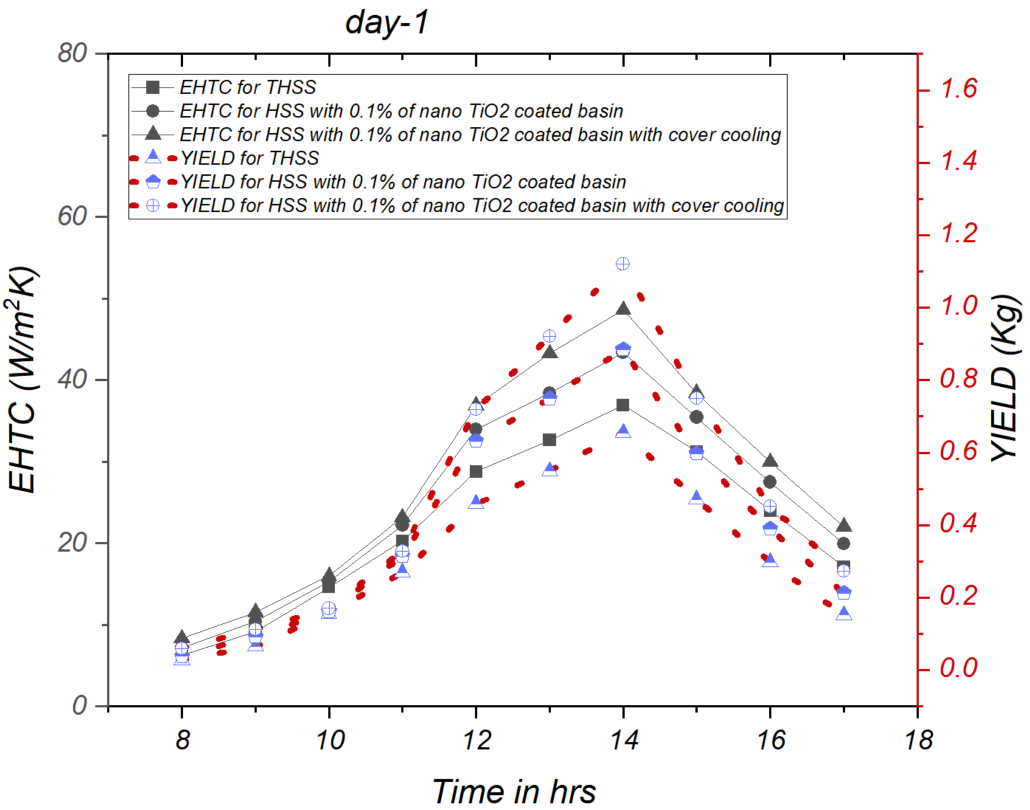

Figure 8. Variations of EHTC and yield of SS on day-1

Figure 9 shows the energy and exergy analysis of THSS, HSS with 0.1% of nano TiO_2 coated basin, and HSS with 0.1% of nano TiO_2 coated basin with cover cooling. The intermittent variations of exergy for the THSS, HSS with 0.1% of nano TiO_2 coated basin, and HSS with 0.1% of nano TiO_2 coated basin with cover cooling are calculated as the ratio of exergy output to exergy input. The highest energy and exergy of THSS are 53.89 and 3.52%, separately. The highest energy and exergy of HSS with 0.1% of nano TiO_2 coated basin are 65.41 and 4.67%, correspondingly. The highest energy and exergy of HSS with 0.1% of nano TiO_2 coated basin with cover cooling are 61.08 and 4.16%, correspondingly. The diurnal average value of energy and exergy of THSS is 28.99 and 1.73%, correspondingly. The daily average value of energy and exergy of HSS with 0.1% of nano TiO_2 coated basin is 42.07 and 2.69%, separately. The diurnal average value of energy and exergy of HSS with 0.1% of nano TiO_2 coated basin with cover cooling is 48.45 and 2.84%, respectively. The highest daily average value of energy and exergy of HSS with 0.1% of nano TiO_2 coated basin with cover cooling is 6.38 and 0.15% higher than HSS with 0.1% of nano TiO_2 coated basin and 19.46 and 1.11% higher than the THSS. The maximum difference between T_w and T_g in the HSS with 0.1% of nano TiO_2 coated basin with cover cooling leads to higher yield and hence increases the exergy and energy when compared to THSS and HSS with 0.1% of nano TiO_2 coated basin. The usage of nano TiO_2 coated basin and nano TiO_2 coated basin with cover cooling in HSS increases the surface area of the basin and results in a higher yield and efficiencies. These results exhibited the efficiency of the proposed modifications to enhance the output of the HSS.

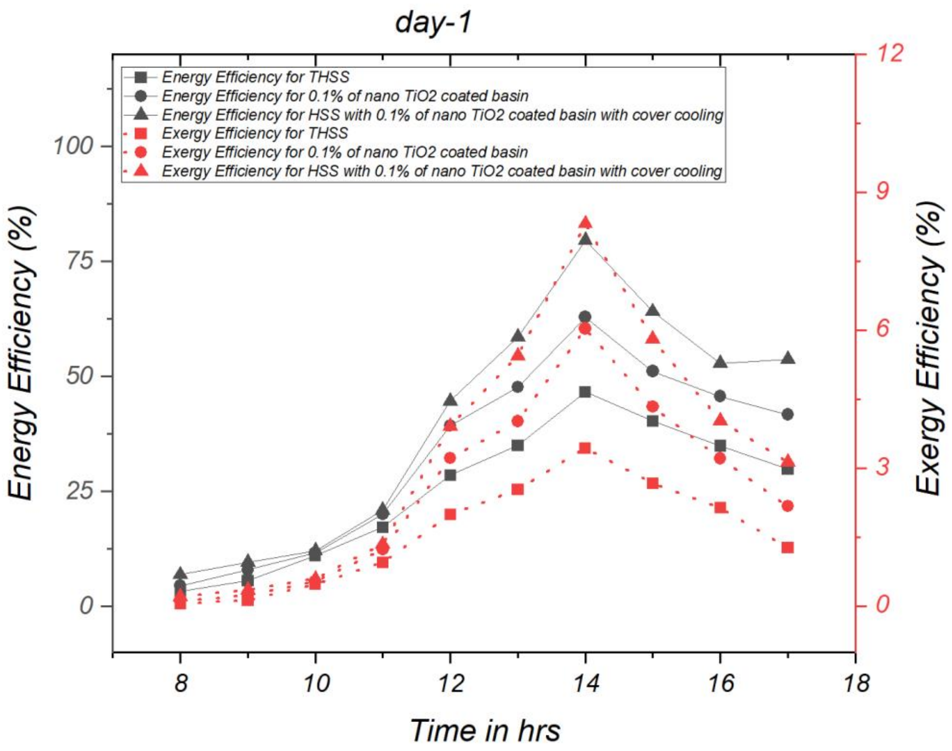

Figure 9. Variations of energy and exergy efficiency of SS on day-1

4.2 performance of THSS, HSS with 0.2% of nano TiO_2 coated basin, and HSS with 0.2% of nano TiO_2 coated basin with cover cooling

Figure 10 represents the intermittent variation of solar radiation, T_a, T_w, and T_g on day-2. The average T_a of day-2 was 33˚C which is comparatively higher than that of day-1. The difference between T_w and T_g in the THSS, HSS with 0.2% of nano TiO_2 coated basin, and HSS with 0.2% of nano TiO_2 coated basin with cover cooling is in the range of 1 to 10 ˚C, 5 to 13 ˚C, and 6 to 16 ˚C, separately. The higher temperature difference between T_w and T_g leads to maximum yield. As per the experiment, the temperature difference between T_w and T_g is more in the HSS with 0.2% of nano TiO_2 coated basin with cover cooling hence yield produced was more. The average solar radiation of day-2 is 684.2 W/m^2. The average T_w of THSS, HSS with 0.2% of nano TiO_2 coated basin, and HSS with 0.2% of nano TiO_2 coated basin with cover cooling is 48.5, 53.2, and 52.2˚C, separately. The average T_g of THSS, HSS with 0.2% of nano TiO_2 coated basin, and HSS with 0.2% of nano TiO_2 coated basin with cover cooling is 42.7, 44.5, and 41.3˚C, separately. The average difference between T_w and T_g of THSS, HSS with 0.2% of nano TiO_2 coated basin, and HSS with 0.2% of nano TiO_2 coated basin with cover cooling is 5.8°C, 8.7°C, and 10.9°C, respectively. It's inferred from Figure 10, that the average T_w and T_g of HSS with 0.2% of nano TiO_2 coated basin with cover cooling is 52.2˚C and 41.3˚C which is 1˚C and 3.2˚C lower than the average T_w and T_g of HSS with of nano TiO_2 coated basin. The drop in temperature is due to the cooling effect of the HSS cover with 0.2% of nano TiO_2 coated basin with cover cooling. But the difference between T_w and T_g is more in the HSS with 0.2% of nano TiO_2 coated basin with cover cooling hence maximum evaporation rate and maximum yield. According to the comparison tests, utilizing nano TiO_2 improves the HSS's performance. From the day-2 experiments also, it is proven that the surface area of HSS with 0.2% of nano TiO_2 coated basin, and HSS with 0.2% of nano TiO_2 coated basin with cover cooling is higher than that of the THSS. Therefore, HSS with TiO_2 nanoparticles has a higher Tw than the Tw of the THSS.

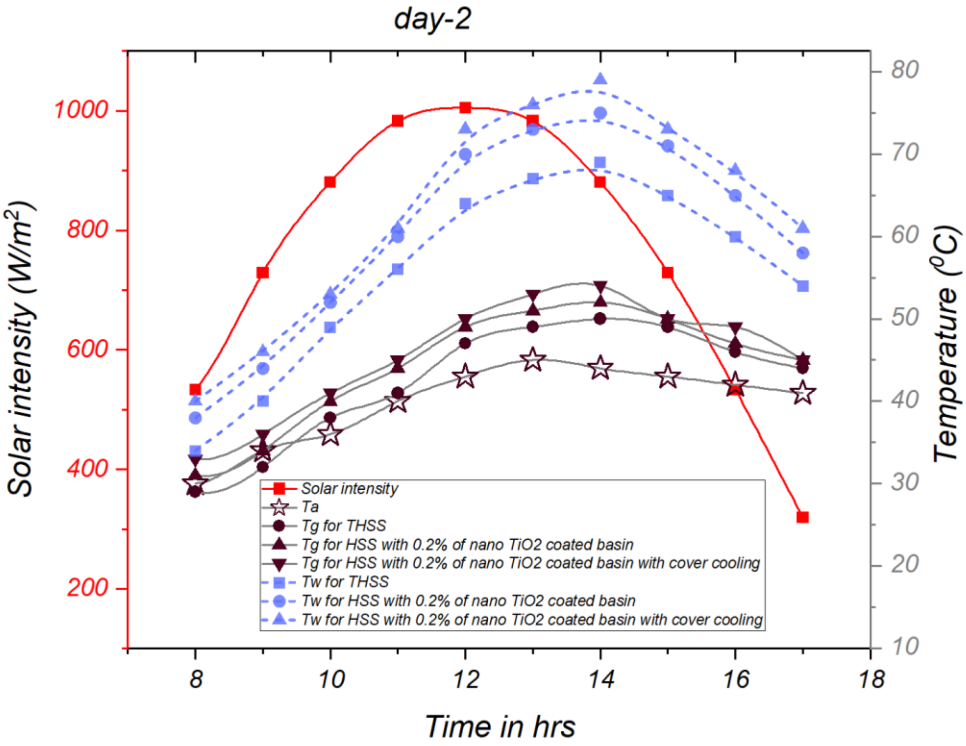

Fig. 10. Variations of solar radiation, T_a, T_w, T_g of SS on day-2

Figure 11 shows the variations of the EHTC and productivity of THSS, HSS with 0.2% of nano TiO_2 coated basin, and HSS with 0.2% of nano TiO_2 coated basin with cover cooling. The maximum EHTC of THSS, HSS with 0.2% of nano TiO_2 coated basin, and HSS with 0.2% of nano TiO_2 coated basin with cover cooling are 35.45, 45.15, and 52.84 W/m^{2}K, correspondingly. The maximum hourly yield of THSS, HSS with 0.2% of nano TiO_2 coated basin, and HSS with 0.2% of nano TiO_2 coated basin with cover cooling is 0.83, 1.0,6, and 1.10 kg, correspondingly. The diurnal yield of THSS, HSS with 0.2% of nano TiO_2 coated basin, and HSS with 0.2% of nano TiO_2 coated basin with cover cooling is 3.75, 5.39, and 5.98 kg, correspondingly. The daily average EHTC of HSS with 0.2% of nano TiO_2 coated basin and HSS with 0.2% of nano TiO_2 coated basin with cover cooling is 45.15 and 52.84 W/m^{2}K, respectively, higher than the THSS. Higher EHTC is found from the graph due to the high temperature in HSS with 0.2% of nano TiO_2 coated basin compared with THSS. Higher EHTC tends to maximize the yield. The nano TiO_2 on the HSS increases Tw, EHTC, and yield compared to the THSS because the absorber plate enhances the thermal conductivity and surface area of the absorber plate.

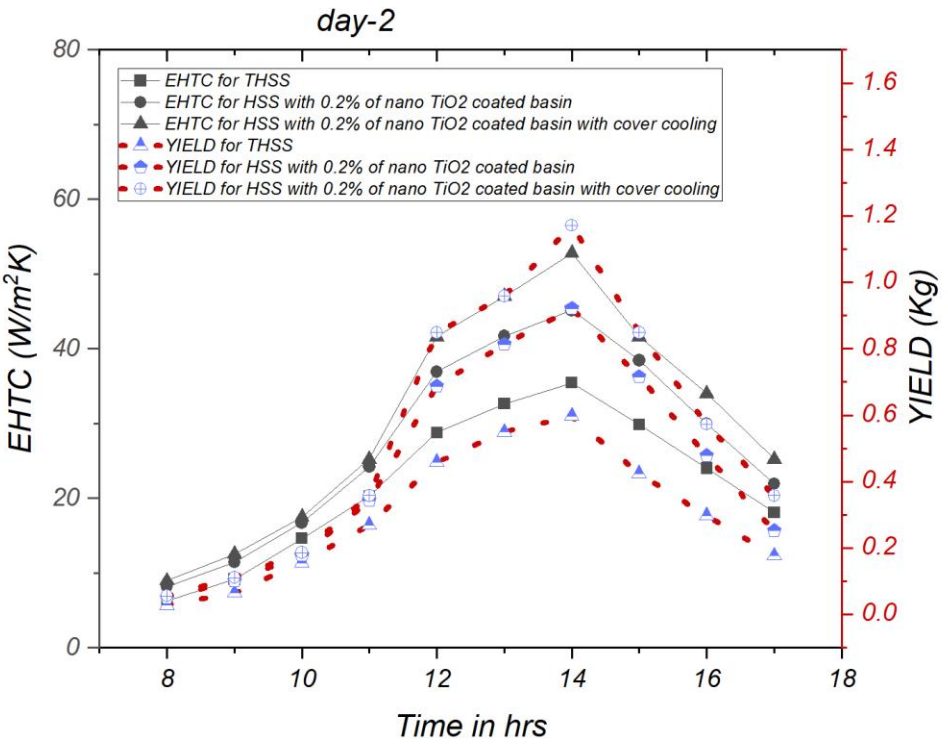

Figure 11. Variations of EHTC and yield of SS on day-2

Figure 12 shows the energy and exergy analysis of THSS, HSS with 0.2% of nano TiO_2 coated basin, and HSS with 0.2% of nano TiO_2 coated basin with cover cooling. The diurnal average value of energy and exergy of THSS is 29.58 and 1.66%, respectively. The daily average value of energy and exergy of HSS with 0.2% of nano TiO_2 coated basin is 48.8 and 3.40%, correspondingly. The diurnal average value of energy and exergy of HSS with 0.2% of nano TiO_2 coated basin with cover cooling is 55.61 and 3.71%, individually. The highest daily average value of energy and exergy of HSS with 0.2% of nano TiO_2 coated basin with cover cooling is 6.81 and 0.31% higher than HSS with 0.2% of nano TiO_2 coated basin and 26.03 and 2.05% higher than the THSS. The maximum difference in temperature between T_w and T_g in the HSS with 0.2% of nano TiO_2 coated basin with cover cooling leads to higher yield and hence increases the exergy and energy when compared to THSS and HSS with 0.2% of nano TiO_2 coated basin. The usage of nano TiO_2 coated basin and nano TiO_2 coated basin with cover cooling in HSS rises the surface area of the basin and results in a higher yield and efficiencies.

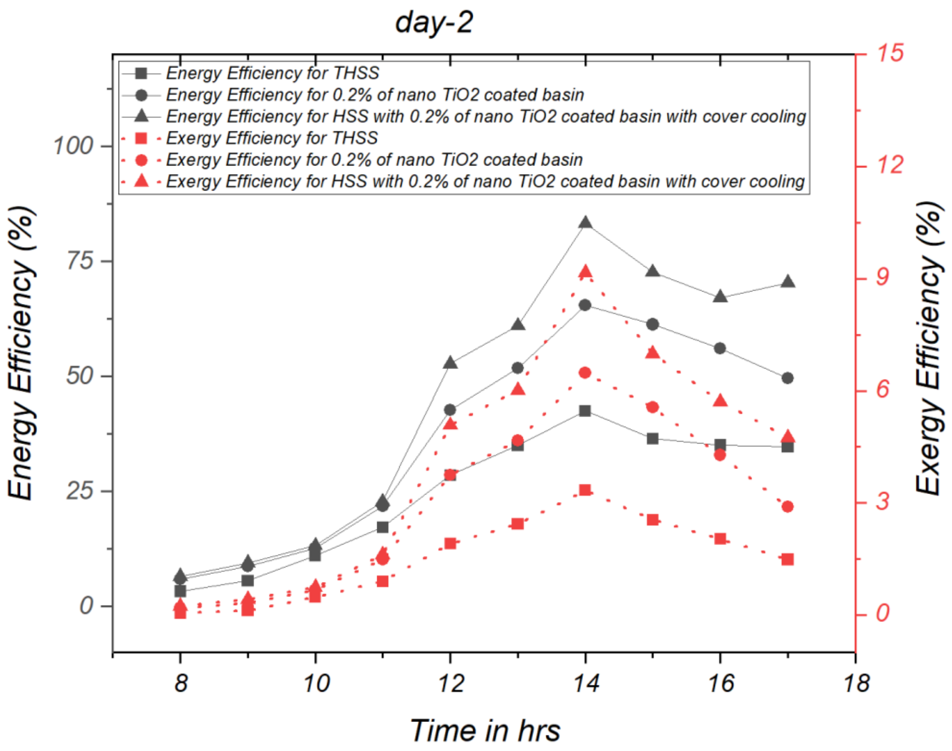

Figure 12. Variations of energy and exergy efficiency of SS on day-2

4.3 performance of THSS, HSS with 0.3% of nano TiO_2 coated basin, and HSS with 0.3% of nano TiO_2 coated basin with cover cooling

Figure 13 represents the intermittent variations of solar radiation, T_a, T_w, and T_g on day-3. The average solar radiation of day-3 is 686.50 W/m^2. The average T_a of day-3 was 32.10˚C. This is comparatively lower than day-1 and day-2. The temperature difference between T_w and T_g in the THSS, HSS with 0.3% of nano TiO_2 coated basin, and HSS with 0.3% of nano TiO_2 coated basin with cover cooling are in the range of 1 to 11˚C, 6 to 14˚C and 7 to 17˚C, separately. The higher difference between T_w and T_g leads to maximum yield. As per the experiment, the temperature difference between T_w and T_g is more in the HSS with 0.3% of nano TiO_2 coated basin with cover cooling hence yield produced was more. The average T_w of THSS, HSS with 0.3% of nano TiO_2 coated basin and HSS with 0.3% of nano TiO_2 coated basin with cover cooling is 48.4˚C, 54.6˚C, and 53.2˚C correspondingly. The average T_g of THSS, HSS with 0.3% of nano TiO_2 coated basin, and HSS with 0.3% of nano TiO_2 coated basin with cover cooling are 42.7, 44.5, and 41.2˚C, individually. The average temperature difference between T_w and T_g of THSS, HSS with 0.3% of nano TiO_2 coated basin, and HSS with 0.3% of nano TiO_2 coated basin with cover cooling is 5.7°C, 10.1°C, and 12°C. It's inferred from Figure 13, that the average T_w and T_g of HSS with 0.3% of nano TiO_2 coated basin with cover cooling is 53.2˚C and 41.2˚C which is 1.4˚C and 3.3˚C lower than the average T_w and T_g of HSS with of nano TiO_2 coated basin. The drop in temperature is due to the cooling effect of the HSS cover with 0.3% of nano TiO_2 coated basin with cover cooling. But the difference between T_w and T_g is more in the HSS with 0.3% of nano TiO2 coated basin with cover cooling hence maximum evaporation and maximum yield. According to the comparison tests, utilizing nano TiO_2 improved the

HSS's performance. From the day-3 experiments, it is proven that the surface area of HSS with 0.3% of nano TiO_2 coated basin, and HSS with 0.3% of nano TiO_2 coated basin with cover cooling is higher than that of the THSS. Therefore, HSS with TiO_2 nanoparticles has a higher Tw than the Tw of the THSS.

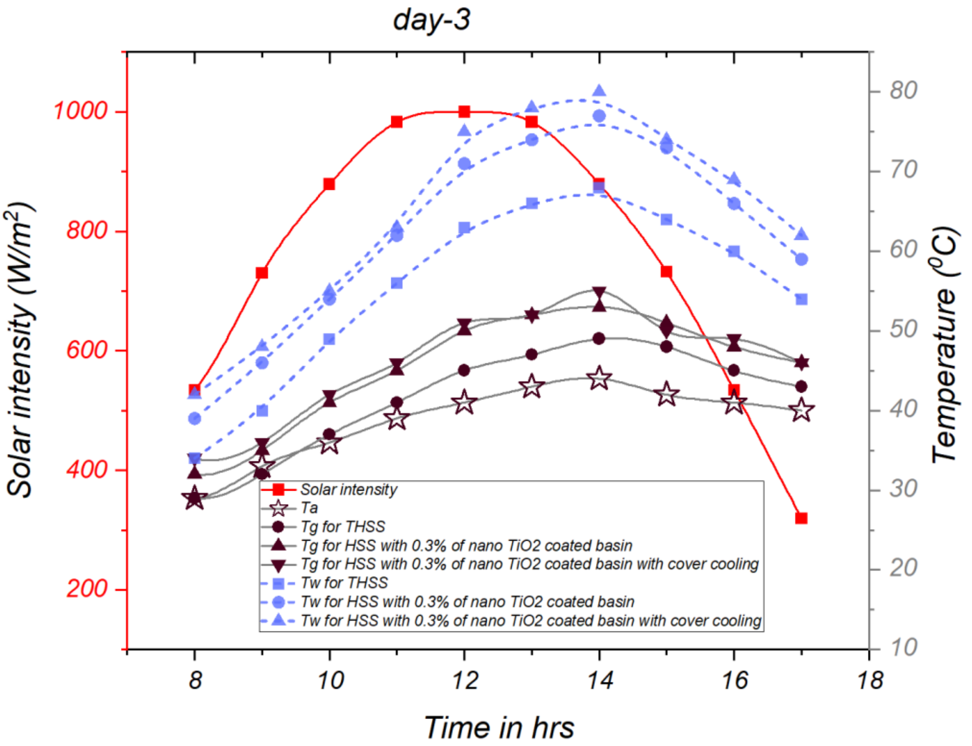

Fig. 13. Variations of solar radiation, T_a, T_w, T_g of SS on day-3

Figure 14 shows the variations of the EHTC and yield of THSS, HSS with 0.3% of nano TiO_2 coated basin, and HSS with 0.3% of nano TiO_2 coated basin with cover cooling. The maximum EHTC of THSS, HSS with 0.3% of nano TiO_2 coated basin, and HSS with 0.3% of nano TiO_2 coated basin with cover cooling are 39.52, 58.86, and 56.85 W/m^2K, respectively. The maximum hourly yield of THSS, HSS with 0.3% of nano TiO_2 coated basin, and HSS with 0.3% of nano TiO_2 coated basin with cover cooling is 0.86, 1.13, and 1.35 kg, correspondingly. The diurnal yield of THSS, HSS with 0.3% of nano TiO_2 coated basin, and HSS with 0.3% of nano TiO_2 coated basin with cover cooling is 3.73, 6.13, and 6.96 kg, individually. The diurnal average EHTC of HSS with 0.3% of nano TiO2 coated basin and HSS with 0.3% of nano TiO_2 coated basin with cover cooling is 38.8 and 36.6 W/m^2K, respectively, higher than the THSS. The diurnal average yield of HSS with 0.3% of nano TiO_2 coated basin with cover cooling is 6.96 which is 0.83 kg higher than HSS with 0.3% of nano TiO_2 coated basin and 3.23 kg higher than the THSS. The maximum daily average of EHTC and yield produced by HSS with 0.3% of nano TiO_2 coated basin is 58.86 W/m^2K and 1.13 kg, respectively. The use of nano-coated basins at concentrations of 0.1, 0.2, and 0.3% in the HSS improves the output of distilled water by 31.27, 50.24, and 67.61% as compared to the THSS. Similarly, the use of nano-coated basin at concentrations of 0.1, 0.2, and 0.3% with glass cooling in the HSS improves the output distilled water by 58.08, 81, and 106.73% as compared to the THSS. Higher EHTC is found from the graph due to the high temperature in HSS with 0.3% of nano TiO2 coated basin compared with THSS. Higher EHTC tends to maximize the yield. The nano TiO_2 on the HSS increases Tw, EHTC, and yield compared to the THSS because the nano-coated absorber plate enhances the thermal conductivity and surface area of the absorber plate.

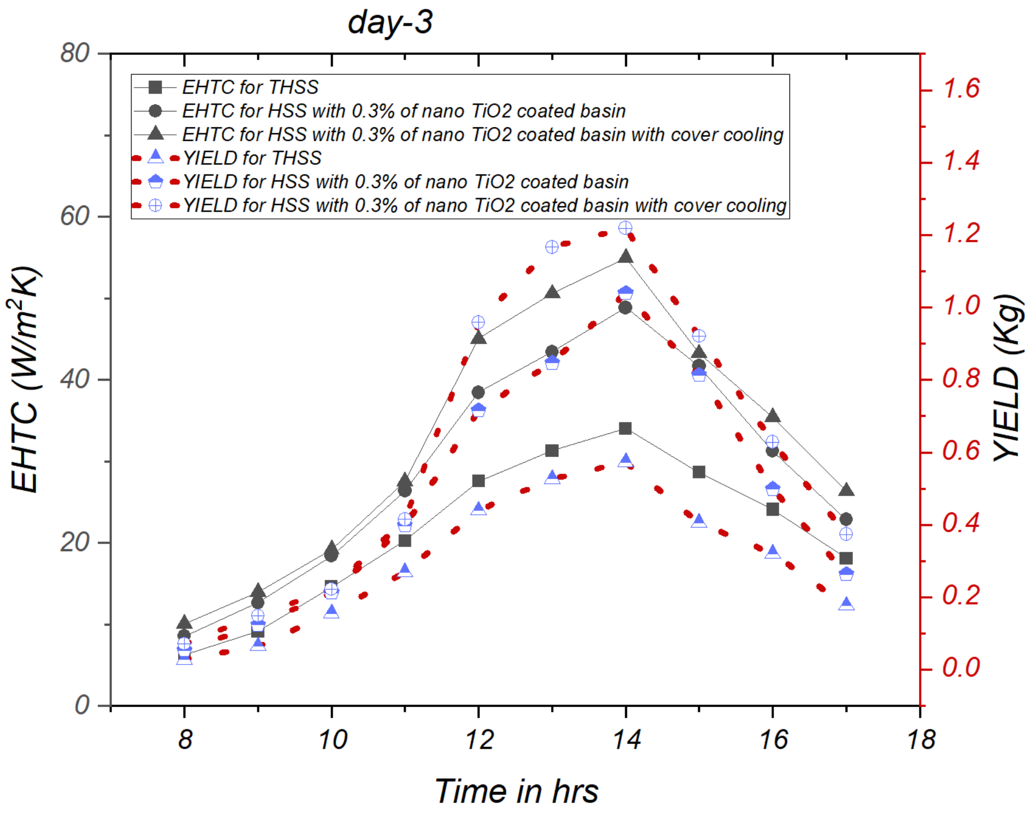

Figure 14. Variations of EHTC and yield of SS on day-3

Figure 15 shows the energy and exergy analysis of THSS, HSS with 0.3% of nano TiO_2 coated basin, and HSS with 0.3% of nano TiO_2 coated basin with cover cooling. The daily average value of energy and exergy of THSS is 29.47 and 1.77%, respectively. The diurnal average value of energy and exergy of HSS with 0.3% of nano TiO_2 coated basin is 56.01 and 4.32%, correspondingly. The diurnal average value of energy and exergy of HSS with 0.3% of nano TiO_2 coated basin with cover cooling is 62.15 and 4.53%, respectively. The highest daily average value of energy and exergy is produced by HSS with 0.3% of nano TiO_2 coated basin with cover cooling is 8.45 and 1.07% higher than HSS with 0.3% of nano TiO_2 coated basin and 34.54 and 3.7% higher than the THSS. The maximum difference between T_w and T_g in the HSS with 0.3% of nano TiO_2 coated basin with cover cooling leads to higher yield and hence increases the exergy and energy when compared to THSS and HSS with 0.3% of nano TiO_2 coated basin. The usage of nano TiO_2 coated basin and nano TiO_2 coated basin with cover cooling in HSS increases the surface area of the basin and results in a higher yield and efficiencies.

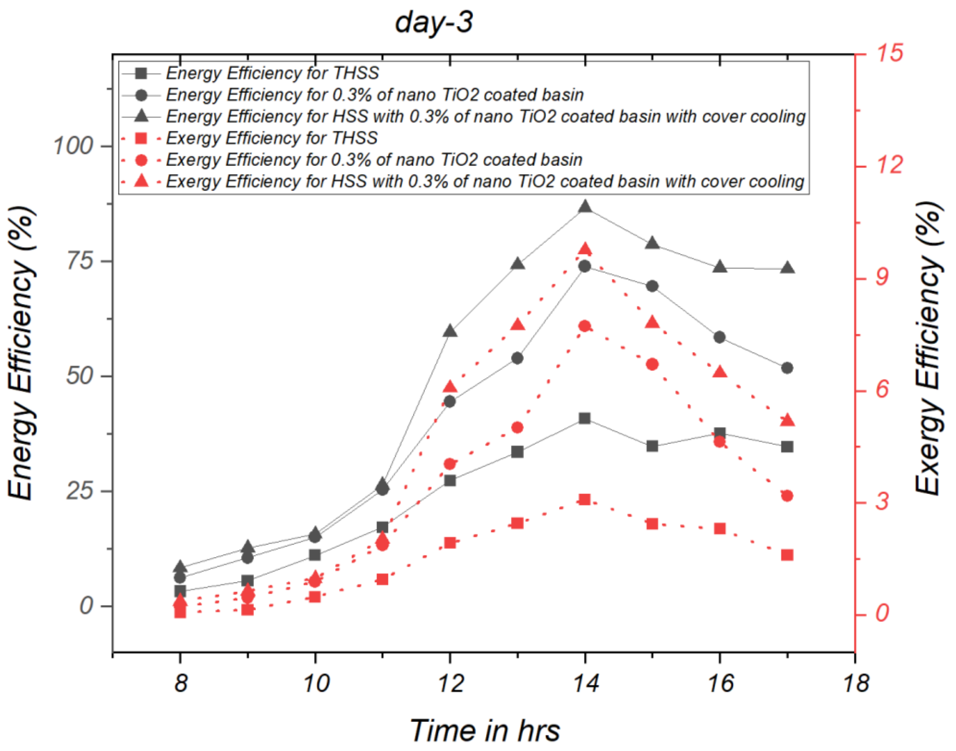

Figure 15. Variations of energy and exergy efficiency of SS on day-3

4.4 Comparison of present studies:

Table 5, 6, and 7 summarizes the Comparison of THSS, HSS with different concentrations of nano TiO_2 coated basin, and HSS with different concentrations of nano TiO_2 coated basin with cover cooling. The yield produced in THSS is 3.7 kg. But yield by the HSS with 0.1% of nano TiO_2 coated basin and HSS 0.1% of nano TiO_2 coated basin with cover cooling is 4.79 kg and 5.48 kg which are 29.6% and 48.01% more than the THSS. The Energy and Exergy efficiency of the HSS with 0.1% of nano TiO_2 coated basin and HSS 0.1% of nano TiO_2 coated basin with cover cooling is 42.07, 2.69, and 48.45, 2.69% which are 55.71%, and 64.84% more than the THSS.

Table 5. Comparison of THSS, HSS with 0.1% of nano TiO_2 coated basin, and HSS with 0.1% of nano TiO_2 coated basin with cover cooling

	THSS	MHSS with 0.1% of nano TiO_2 coated basin	MHSS 0.1% of nano TiO_2 coated basin with cover cooling
Yield	3.7	4.79	5.48
% improvement	---	29.60	48.01
EHTC	26.35	30.18	29.21
% improvement	---	14.5	10.83

Energy	28.99	42.07	48.45
% improvement	---	45.11	67.10
Exergy	1.73	2.69	2.69
% improvement	---	55.71	64.84

The yield produced in THSS is 3.75. But yield by the HSS with 0.2% of nano TiO_2 coated basin and HSS 0.2% of nano TiO_2 coated basin with cover cooling is 43.76% and 59.37% more than the conventional THSS. The Energy and Exergy produced by the HSS with 0.2% of nano TiO_2 coated basin and HSS 0.2% of nano TiO_2 coated basin with cover cooling is 48.80, 3.4, and 55.61, 3.71% which are 105.2%, and 123.8% more than the THSS.

Table 6. Comparison of THSS, HSS with 0.2% of nano TiO_2 coated basin, and HSS with 0.2% of nano TiO_2 coated basin with cover cooling

	THSS	MHSS with 0.2% of nano TiO_2 coated basin	MHSS 0.2% of nano TiO_2 coated basin with cover cooling
Yield	3.75	5.39	5.98
% improvement	--	43.76	59.37
EHTC	25.72	35.51	34.44
% improvement	--	38.06	33.91
Energy	29.58	48.80	55.61
% improvement	--	64.97	87.98
Exergy	1.66	3.40	3.71
% improvement	--	105.20	123.80

The yield produced in THSS is 3.73. But yield by the HSS with 0.3% of nano TiO_2 coated basin and HSS 0.3% of nano TiO_2 coated basin with cover cooling is 6.13 and 6.96 kg which is 64.34% and 86.67% more than the THSS. The energy and exergy efficiency of the HSS with 0.3% of nano TiO_2 coated basin and HSS with 0.3% of nano TiO_2 coated basin with cover cooling is 56.01, 4.32, and 62.15, 4.53 which are 143.49% and 155.7% more than the conventional THSS.

An increase in the concentration of nanoparticles resulted in higher surface area and high solar intensity absorption capacity which resulted in increases in the yield and hence higher efficiencies. The HSS with 0.3% of nano TiO_2 coated basin produces 64.34% improvement and the HSS 0.3% of nano TiO_2 coated basin with cover cooling produces 86.67% than the THSS. Hence increase in the concentration of nanoparticle coating with cover cooling increases the yield and hence the efficiencies.

Table 7. Comparison of THSS, HSS with 0.3% of nano TiO_2 coated basin, and HSS with 0.3% of nano TiO_2 coated basin with cover cooling

	THSS	MHSS with 0.3% of nano TiO_2 coated basin	MHSS 0.3% of nano TiO_2 coated basin with cover cooling
Yield	3.73	6.13	6.96
% improvement	--	64.34	86.67
EHTC	25.57	38.8	36.6
% improvement	--	51.73	43.14
Energy	29.47	56.01	62.15
% improvement	--	90.06	110.90
Exergy	1.77	4.32	4.53
% improvement	--	143.49	155.7

4.5 Comparison of the present study with published similar works

In Table 8, our results are compared with already existing works with hemispherical-based solar desalination systems. From Table 5, it can be noticed that output of HSS with PCM [5] is minimum with a value equal to 29.84%. However, for the HSS with convex absorber basin, wick, and PCM, it is maximum with a value equal to 87.06% [4].

Table 8. Comparison of similar studies

Author(s) and Reference	Absorbers used	Increased (%)
Our results	- 0.3% of Nano-TiO_2 - 0.3% of Nano-TiO_2 and cooling of the glass cover 2.5 L/h	61.84 80.26
Abdelgaied et al. [63]	-PCM -0.3% of Nano -CuO -PCM and 0.3% of Nano-CuO	29.17 60.42 80.21
Kabeel et al. [64]	- V-corrugated circular basin and reversed solar collector	68.82
Beggas et al. [65]	- Aluminum waste	48.19
Attia et al. [66]	- Convex absorber basin and wick - Convex absorber basin, Wick and PCM	62.35 87.06
Ravishankar et al. [67]	- PCM - Mixed Nano- Al_2O_3 with PCM	27.84 71.13

5. Economic Assessment

5.1. **Accumulated daily** productivity

Table 9 nations the accumulated daily productivity of HSS without and with nano-TiO_2 of various concentrations with a cooling plastic cap at a constant flow recorded on experiments days September 28, 29, and 30, 2022 for a period of 10 hours. It can be seen that employing HSS-TiO2&0.3%+2.5 L/h enabled the maximum improvement in daily yield to reach 80.26%.

Table 9: daily output of THSS, HSS-TiO_2, and HSS- TiO_2 with cooling plastic cap at a constant flow at 2.5 L/h recorded during trial hours.

Experiment	Date	THSS (L/m^2)	HSS- TiO_2 (L/m^2)			HSS-TiO_2 and cooling of the glass cover 2.5 L/h (L/m^2)			Improvement rate (%)
			0.1%	0.2%	0.3%	0.1%	0.2%	0.3%	
One	28/09/2022	3.1	4.07	-	-				31.27
						4.9	-	-	58.08
Two	29/09/2022	3.02	-	4.54	-				50.24
						-	5.47	-	80.93
Three	30/09/2022	2.96	-	-	4.96				67.61
						-	-	6.12	106.73

5.2. Economic analysis

A comprehensive cost analysis is performed for all the HSS. **Table 10** displays the time takes to recover the total cost of THSS, HSS with 0.1% of nano TiO_2 coated basin, and HSS with 0.1% of nano TiO_2 coated basin with cover cooling, THSS, HSS with 0.2% of nano TiO_2 coated basin, and HSS with 0.2% of nano TiO_2 coated basin with cover cooling and THSS, HSS with 0.3% of nano TiO_2 coated basin, and HSS with 0.3% of nano TiO_2 coated basin with cover cooling, respectively. The payback period of 19 days is obtained for the HSS-TiO2C&0.3%+2.5 L/h.

Table 10: Manufacturing cost of the different HSS

(1$=132.78 DZD, 1€=156.03 DZD)

	THSS	HSS-TiO2			HSS-TiO2		
		0.1%	0.2%	0.3%	0.1% +2.5L/h	0.2% +2.5L/h	0.3% +2.5L/h
total cost of production (DZD)	9000	9000	9000	9000	9000	9000	9000
The price of nanoparticle of TiO_2 (DZD)	-	15	30	45	15	30	45
The price of spray water (DZD)	-		-		-	30	30
Cost of maintenance (DZD)	50	50	50	50	50	50	50
Total cost (DZD)	9050	9065	9080	9095	9095	9110	9125
the volume of water generated each day ($kg/m^2/day$)	3.1	4.07	4.54	4.96	4.9	5.47	6.12
The price of distilled water per liter in the market (DZD)	60	60	60	60	60	60	60
The cost of producing water per day (DZD)	186	244.2	272.4	297.6	294	328.2	367.2
Recovery period (days)	49	37	33	30	31	28	25

Conclusions

This study focuses on adopting varying concentrations of nano- TiO_2 (0.1, 0.2, and 0.3 percent) with a cooling plastic cap at a constant flow at 2.5 L/h, to improve the productivity of HSS experimentally. The experiments were conducted on September 28, 29, and 30, 2022 for a period of 10 hours. The test outcomes led to the following conclusions:

1. Nano-TiO_2 and Cooling the plastic cap significantly improves the efficiency of the HSS.
2. The daily yield following from THSS and HSS with nano-TiO_2 at various concentrations (0.1, 0.2, and 0.3%) are 3.1, 4.07, 4.54, and 4.96 $kg/m^2/day$, respectively.
3. The daily yield resulting from HSS with nano-TiO_2 at various concentrations (0.1, 0.2, and 0.3%) with cooling plastic cap at a constant flow at 2.5 L/h are 4.9, 5.47, and 6.12 $kg/m^2/day$.
4. The HSS with 0.3 percent TiO_2 with a cooling plastic cap at a constant flow at 2.5 L/h achieved the highest yield as compared to the HSS with 0.1 and 0.2 percent TiO_2 with a cooling plastic cap at a constant flow at 2.5 L/h.
5. When using HSS with 0.1, 0.2, and 0.3 percent TiO_2, the yield was improved by 31.27, 50.2, and 67.6%, respectively as compared to THSS.
6. When using HSS with 0.1, 0.2, and 0.3 percent TiO_2 with a cooling plastic cap at a constant flow at 2.5 L/h, improved the yield by 58.08, 81, and 106.7%, respectively, compared to THSS.

7. Daily energy efficiency for the HSS with a nano-coated basin was found to be 33.24, 37.61, and 41%, while daily exergy efficiency was found to be 2.52, 3.03, and 3.47%, respectively.
8. The HSS with a nano-coated basin at concentrations of 0.1, 0.2, and 0.3% with glass cooling was found to have daily energy efficiencies of 40.34, 46, and 51%, respectively, while daily exergy efficiencies were 3.32, 4.07, and 4.71%.
9. 51 days are needed for the payback period to recover the complete cost of THSS, whereas 25 days for HSS-TiO2&0.3%+2.5L/h. This indicates that the HSS-TiO2&0.3%+2.5L/h is the best economical HSS.

Finally, by increasing the concentration of TiO_2 nanoparticles and cooling the plastic cap, the output of an HSS can be greatly increased.

Nomenclature

SS	Solar Still
SSSS	Single Slope Solar Still
THSS	Traditional Hemispherical Solar Still
EHTC	Evaporative Heat Transfer Coefficient

Appendix-1:

Experimental errors:

Table 3: Errors of the used devices

Device name	Measuring parameter	Range	Accuracy	Error
Solar meter	solar radiation	0-3500 W/m^2	±10 W/m^2	± 3.5 %
Calibrated flask	Hourly yield	0-1500 ml	± 10 ml	± 1.5%
Thermocouple	temperature	0 to 600 °C	± 0.1 °C	±1.5%
Digital indicator	display	-	-	-

Uncertainty analysis [69-71]

If there is a possibility of instrument error, the total level of uncertainty during the investigation will alter. It is written as,

$$R_m = \sqrt{\left(\frac{\partial m}{\partial h} R_h\right)^2} \quad (1)$$

The amount of uncertainty in calculating the daily efficiency of the THSS, HSS with different nano TiO_2 coated basin, and HSS with different nano TiO_2 coated basins with cover cooling is calculated by,

$$R_\eta = \sqrt{\left(\frac{\partial \eta}{\partial m} R_m\right)^2 + \left(\frac{\partial \eta}{\partial I(t)} R_{I(t)}\right)^2} \quad (2)$$

There are 1.5, 3.5, and 1.5% estimated uncertainties for temperature, sun intensity, and yield, respectively. Equation (2) is used to calculate the uncertainty error for daily thermal efficiency, and the result is 2.1%.

Appendix-2:

Figures 16 and 17 shows the formulas to find the energy and exergy efficiency of the THSS, HSS with different nano TiO_2 coated basin, and HSS with different nano TiO_2 coated basins with cover cooling,

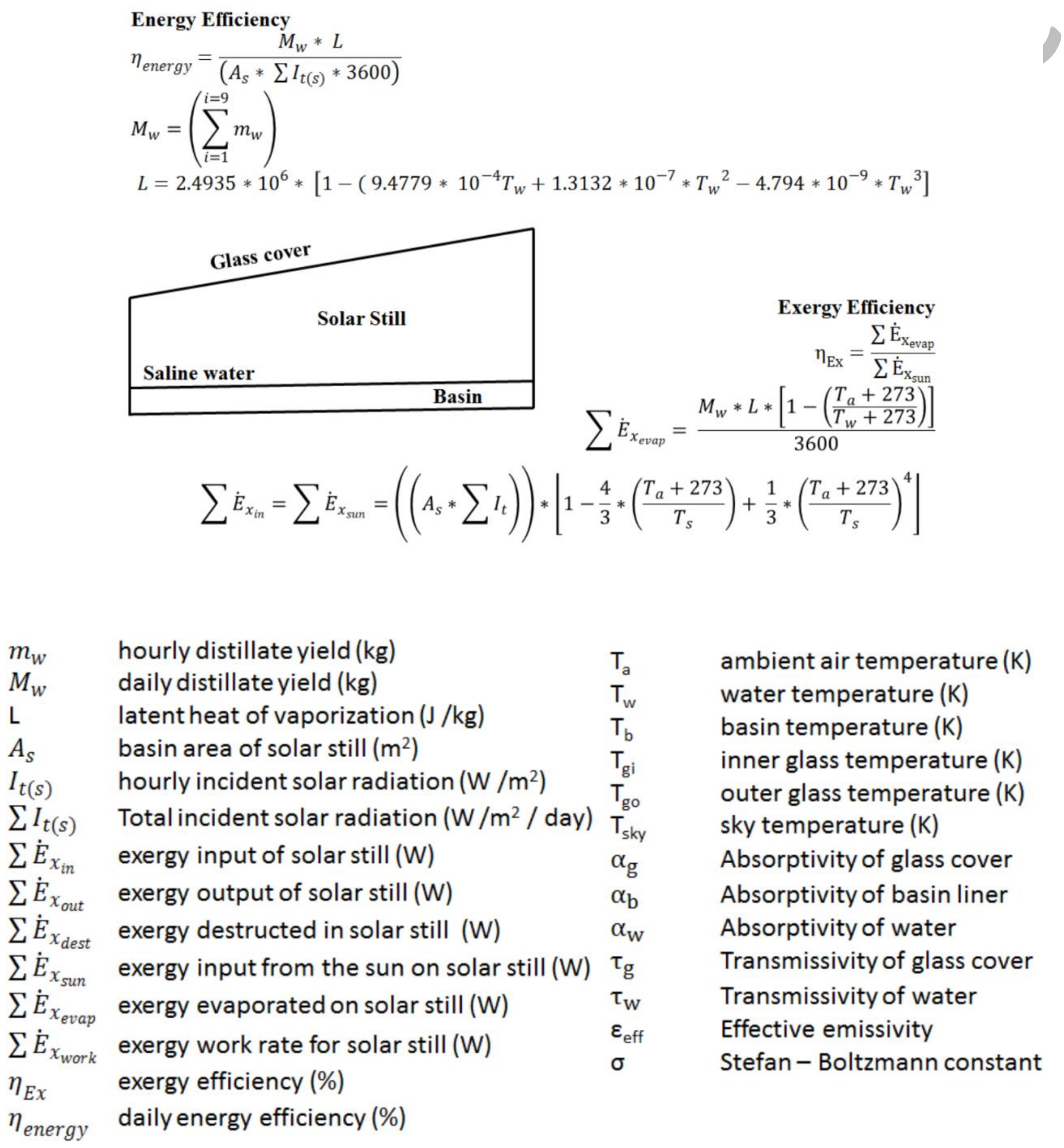

Fig 16 Energy efficiency [68]

Glass Cover - Exergy Destruction

$$E_{x_{des.,g}} = \alpha_g E_{x_{sun}} + E_{x_{t,w-g}} - E_{x_{t,g-a}}$$

$$E_{x_{t,g-a}} = E_{x_{c,g-a}} + E_{x_{r,g-a}}$$

$$E_{x_{r,g-a}} = h_{r,g-a}(T_{go} - T_a)\left[1 + \frac{1}{3}\left(\frac{T_a}{T_{go}}\right)^4 - \frac{4}{3}\left(\frac{T_a}{T_{go}}\right)\right]$$

$$E_{x_{c,g-a}} = h_{c,g-a}(T_{go} - T_a)\left(1 - \frac{T_a}{T_{go}}\right)$$

$$h_{r,g-a} = \frac{\varepsilon_{eff}\,\sigma\,(T_{go}^{4} - T_{sky}^{4})}{T_{go} - T_{sky}} \qquad T_{sky} = 0.0552\,T_a^{1/5}$$

$$h_{c,g-a} = 5.7 + 3.8\,V$$

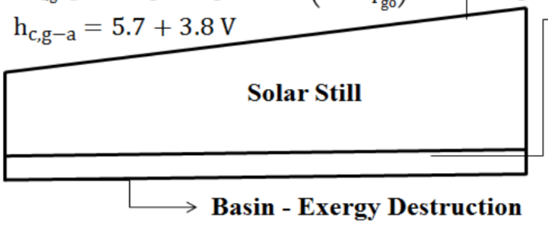

Saline water - Exergy Destruction

$$E_{x_{des.,w}} = (\tau_g \alpha_w)E_{x_{sun}} + E_{x_w} - E_{x_{t,w-g}}$$

$$E_{x_{t,w-g}} = E_{x_{e,w-g}} + E_{x_{c,w-g}} + E_{x_{r\,w-g}}$$

$$E_{x_{e,w-g}} = h_{e,w-g}(T_w - T_{gi})\left(1 - \frac{T_a}{T_w}\right)$$

$$h_{e,w-g} = 0.016273\, h_{c,w-g}\frac{P_w - P_{gi}}{T_w - T_{gi}}$$

$$P(T) = exp\left[25.317 - \frac{5144}{T}\right]$$

$$E_{x_{c,w-g}} = h_{c,w-g}(T_w - T_{gi})\left(1 - \frac{T_a}{T_w}\right)$$

$$h_{c,w-g} = 0.884\left[T_w - T_{gi} + \frac{(P_w - P_{gi})T_w}{268900 - P_w}\right]^{1/3}$$

Basin - Exergy Destruction

$$E_{x_{des.,b}} = (\tau_g \tau_w \alpha_b)E_{x_{sun}} - (E_{x_w} + E_{x_{ins.}})$$

$$E_{x_{sun}} = I_t\left[1 + \frac{1}{3}\left(\frac{T_a}{T_s}\right)^4 - \frac{4}{3}\left(\frac{T_a}{T_s}\right)\right]$$

$$E_{x_w} = h_w(T_b - T_w)\left(1 - \frac{T_a}{T_b}\right)$$

$$E_{x_{ins.}} = h_b(T_b - T_a)\left(1 - \frac{T_a}{T_b}\right)$$

$$h_{r,w-g} = \varepsilon_{eff}\,\sigma\,(T_w^{2} + T_{gi}^{2})(T_w + T_{gi}) \qquad E_{x_{r,w-g}} = h_{r,w-g}(T_w - T_{gi})\left[1 + \frac{1}{3}\left(\frac{T_a}{T_w}\right)^4 - \frac{4}{3}\left(\frac{T_a}{T_w}\right)\right]$$

$E_{x_{des.,b}}$	exergy destruction from basin liner (W / m²)
$E_{x_{des.,w}}$	exergy destruction from saline water (W / m²)
$E_{x_{des.,g}}$	exergy destruction from glass cover (W / m²)
$E_{x_{ins.}}$	exergy loss through insulation (W / m²)
E_{x_w}	exergy utilized to heat saline water (W / m²)
$E_{x_{t,w-g}}$	total exergy associated with saline water and glass cover (W / m²)
$E_{x_{e,w-g}}$	exergy associated with saline water and glass cover through evaporation (W / m²)
$E_{x_{c,w-g}}$	exergy associated with saline water and glass cover through convection (W / m²)
$E_{x_{r,w-g}}$	exergy associated with saline water and glass cover through radiation (W / m²)
$E_{x_{t,g-a}}$	total exergy associated with glass cover and atmosphere (W / m²)
$E_{x_{c,g-a}}$	exergy associated with glass cover and atmosphere through convection (W / m²)
$E_{x_{r,g-a}}$	exergy associated with glass cover and atmosphere through radiation (W / m²)
h_w	convective heat transfer between basin liner and water (W / m² K)
h_b	overall heat transfer between basin liner and atmosphere (W / m² K)
$h_{e,w-g}$	evaporative heat transfer coefficient between saline water and glass cover (W / m² K)
$h_{c,w-g}$	convective heat transfer coefficient between saline water and glass cover (W / m² K)
$h_{r,w-g}$	radiative heat transfer coefficient between saline water and glass cover (W / m² K)
$h_{c,g-a}$	convective heat transfer coefficient between glass cover and atmosphere (W / m² K)
$h_{r,g-a}$	radiative heat transfer coefficient between glass cover and atmosphere (W / m² K)
V	wind velocity in (m / s)

Fig. 17 Exergy efficiency [68]

“Conflict of interest

On behalf of all authors, the corresponding author states that there is no conflict of interest.”

References

1. Attia, M. E. H., Kabeel, A. E., Abdelgaied, M., Abdelaziz, G. B. A., comparative study of hemispherical solar stills with various modifications to obtain modified and inexpensive still models, Environ. Sci. Pollut. Res., 28(39): 55667-55677 (2021).

2. Younis, O., Hussein, A. K., Attia, M. E. H., Aljibori, H. S. S., Kolsi, L., Togun, H., ... Jirawattanapanit, A., Comprehensive review on solar stills—Latest developments and overview, Sustainability, 14(16): 10136 (2022).

3. Attia, M. E. H., Hussein, A. K., Radhakrishnan, G., Vaithilingam, S., Younis, O., Akkurt, N., Energy, exergy and cost analysis of different hemispherical solar distillers: A comparative study, *Sol. Energy Mater Sol. Cells*, *252:* 112187 (2023).

4. Attia, M. E. H., Abdelgaied, M., Abdullah, A., A comparative study of the effect of internal reflectors on a performance of hemispherical solar distillers: energy, exergy, and economic analysis, *Sustain. Energy Technol. Assess, 47:* 101465 (2021).

5. Attia, M. E. H., Elaloui, E., Abdelgaied, M., Abdullah, A., Experimental study on improving the yield of hemispherical distillers using CuO nanoparticles and cooling the glass cover, *Sol. Energy Mater Sol. Cells, 235:* 111482 (2022).

6. Younis, O., Hussein, A. K., Attia, M. E. H., Rashid, F. L., Kolsi, L., Biswal, U., ... Alazzam, A., Hemispherical solar still: Recent advances and development, *Energy Rep*, *8:* 8236-8258 (2022).

7. Attia, M. E. H., El-Maghlany, W. M., Abdelgaied, M., Elharidi, A. M., Finest concentration of phosphate grains as energy storage medium to improve hemispherical solar distillate: An Experimental study, *Alex. Eng. J.*, *61*(7): 5573-5583 (2022).

8. Attia, M. E. H., Abdelgaied, M., Abdel-Aziz, M. M., Bellila, A., Abdullah, A., Optimal size of black gravel as energy storage materials for performance improvement of hemispherical distillers, *J. Energy Storage*, *43*: 103196 (2021).

9. Abdelgaied, M., Attia, M. E. H., Kabeel, A. E., Zayed, M. E., Improving the thermo-economic performance of hemispherical solar distiller using copper oxide nanofluids and phase change materials: Experimental and theoretical investigation, *Sol. Energy Mater Sol. Cells*, *238:* 111596 (2022).

10. Kabeel, A. E., Attia, M. E. H., Zayed, M. E., Abdelgaied, M., Abdullah, A. S., El-Maghlany, W. M., Performance enhancement of a v-corrugated basin hemispherical solar distiller combined with reversed solar collector: An experimental approach, Renew. Energy, *190*: 330-337 (2022).

11. Kaushal, A., Solar stills: A review, Renew. Sust. Energ. Rev., *14*(1): 446-453 (2010).

12. El-Sebaii, A. A., El-Bialy, E., Advanced designs of solar desalination systems: A review, Renew. Sust. Energ. Rev., *49:* 1198-1212 (2015).

13. Prakash, P., Velmurugan, V., Parameters influencing the productivity of solar stills–A review, Renew. Sust. Energ. Rev., *49:* 585-609 (2015).

14. Rufuss, D. D. W., Iniyan, S., Suganthi, L., & Davies, P. A., Solar stills: A comprehensive review of designs, performance and material advances, Renew. Sust. Energ. Rev., *63:* 464-496 (2016).

15. Hussein, A. K., Kolsi, L., Younis, O. B. A. I., Li, D., Ali, H. M., Afrand, M. A. S. O. U. D., Using of nanotechnology concept to enhance the performance of solar stills-recent advances and overview, *J. Eng. Sci. Technol.*, *15*(6): 3991-4031 (2020).

16. Jobrane, M., Kopmeier, A., Kahn, A., Cauchie, H. M., Kharroubi, A., Penny, C., Internal and external improvements of wick type solar stills in different configurations for drinking water production–A review, *Groundw. Sustain. Dev.*, *12*: 100519 (2021).

17. Chauhan, V. K., Shukla, S. K., Tirkey, J. V., & Rathore, P. K. S., A comprehensive review of direct solar desalination techniques and its advancements, *J. Clean. Prod. 284*: 124719 (2021).

18. Alnaimat, F., Ziauddin, M., & Mathew, B., A review of recent advances in humidification and dehumidification desalination technologies using solar energy, *Desalination*, *499*: 114860 (2021).

19. Attia, M. E. H., Kabeel, A. E., Abdelgaied, M., Driss, Z., Productivity enhancement of traditional solar still by using sandbags of El Oued, Algeria, *Heat Transf.*, *50*(1): 768-783 (2021)

20. Attia, M. E. H., Kabeel, A. E., Abdelgaied, M., Essa, F. A., Omara, Z. M., Enhancement of hemispherical solar still productivity using iron, zinc and copper trays, *Sol Energy*, *216*: 295-302 (2021).

21. Attia, M. E. H., Driss, Z., Manokar, A. M., Sathyamurthy, R., Effect of aluminum balls on the productivity of solar distillate, *J. Energy Storage*, *30*: 101466 (2020).

22. Kabeel, A. E., Harby, K., Abdelgaied, M., Eisa, A., A comprehensive review of tubular solar still designs, performance, and economic analysis, *J. Clean. Prod.*, *246*: 119030 (2020).

23. Kabeel, A. E., Harby, K., Abdelgaied, M., Eisa, A., Performance of the modified tubular solar still integrated with cylindrical parabolic concentrators, *Sol Energy*, 204: 181-189 (2020).

24. Ketabchi, F., Gorjian, S., Sabzehparvar, S., Shadram, Z., Ghoreishi, M. S., Rahimzadeh, H., Experimental performance evaluation of a modified solar still integrated with a cooling system and external flat-plate reflectors, *Sol Energy*, *187:* 137-146 (2019).

25. Ismail, B. I., Design and performance of a transportable hemispherical solar still, *Renew. Energy*, *34*(1): 145-150 (2009).

26. Arunkumar, T., Jayaprakash, R., Denkenberger, D., Ahsan, A., Okundamiya, M. S., Tanaka, H., Aybar, H. Ş. An experimental study on a hemispherical solar still, *Desalination*, *286*: 342-348 (2012).

27. Raju, J. D., Vaibhav, T. L. V., Chaitanya, C. S., Kotebavi, V., An Experimental investigation on Hemispherical Basin Solar Still coupled with Heat Pipes, Evacuated Tubes& Paraboloid Concentrator. In *IOP Conference Series: Materials Science and Engineering* (Vol. 225, No. 1, p. 012056) IOP Publishing (2017, August).

28. Abu-Hijleh, B. A. Enhanced solar still performance using water film cooling of the glass cover, *desalination*, *107*(3): 235-244 (1996).

29. Mousa, H. A., Water film cooling over the glass cover of a solar still including evaporation effects, Energy, 22(1): 43-48 (1997).

30. Khan, M. Z., Nawaz, I., Tiwari, G. N., Meraj, M., Effect of top cover cooling on the performance of hemispherical solar still, *Mater. Today: Proc.*, *38*: 384-390 (2021).

31. Sahota, L., Tiwari, G. N., Effect of Al2O3 nanoparticles on the performance of passive double slope solar still, *Sol Energy*, *130*: 260-272 (2016).

32. Sahota, L., Tiwari, G. N., Effect of Al2O3 and TiO2-water based nanofluids on heat transfer coefficients of passive double slope solar still, *Int J Energy Environ Econ*, *24*(1): 3 (2016).

33. Madhu, B., Balasubramanian, E., Nagarajan, P. K., Ravishankar, S., Kabeel, A. E., Arunkumar, T., Mageshbabu, D., Improving the yield of fresh water from conventional and stepped solar still with different nanofluids, Desalin. Water Treat., *100*: 243-249 (2017).

34. Kabeel, A. E., Omara, Z. M., Essa, F. A., Abdullah, A. S., Arunkumar, T., Sathyamurthy, R., Augmentation of a solar still distillate yield via absorber plate coated with black nanoparticles, *Alex. Eng.J* , *56*(4): 433-438 (2017).

35. Kabeel, A. E., Omara, Z. M., Essa, F. A., Enhancement of modified solar still integrated with external condenser using nanofluids: An experimental approach, *Energy Convers. Manag.*, *78:* 493-498 (2014).

36. Kabeel, A. E., Omara, Z. M., Essa, F. A., Improving the performance of solar still by using nanofluids and providing vacuum, *Energy Convers. Manag.*, *86:* 268-274 (2014).

37. Shanmugan, S., Palani, S., Janarthanan, B., Productivity enhancement of solar still by PCM and Nanoparticles miscellaneous basin absorbing materials, *Desalination*, *433:* 186-198 (2018).

38. Subhedar, D. G., Chauhan, K. V., Patel, K., Ramani, B. M., Performance improvement of a conventional single slope single basin passive solar still by integrating with nanofluid-based parabolic trough collector: an experimental study, Mater. Today: Proc., *26*: 1478-1481 (2020).

39. Kabeel, A. E., Sathyamurthy, R., Sharshir, S. W., Muthumanokar, A., Panchal, H., Prakash, N., ... El Kady, M. S., Effect of water depth on a novel absorber plate of pyramid solar still coated with TiO2 nano black paint, *J. Clean. Prod.*, *213*: 185-191 (2019).

40. Shanmugan, S., Essa, F. A., Gorjian, S., Kabeel, A. E., Sathyamurthy, R., Manokar, A. M., Experimental study on single slope single basin solar still using TiO2 nano layer for natural clean water invention, *J. Energy Storage*, *30*: 101522 (2020).

41. Shayanmehr, M., Mahdavi, H., Mechanical modeling of a high performance solar desalination system based on a three step approach. *Iran. J. Chem. Chem. Eng.*. (2022).

42. Norouzi, N., & Bozorgian, A. (2023). Energy and exergy analysis and optimization of a Pentageneration (cooling, heating, power, water and hydrogen). Iran. J. Chem. Chem. Eng.

43. Elangovan, R., Seeram, S. R., Radha Krishnan, B., Vijayan, V., Experimental Investigation and Parameter Analysis of Solar Still with the Different Wick Materials, *Iran. J. Chem. Chem. Eng.*, *41*(1): 304-309 (2022).

44. Bahrami, M., Avargani, V. M., Bonyadi, M., Comprehensive experimental and theoretical study of a novel still coupled to a solar dish concentrator, *Appl. Therm. Eng.*, *151*: 77-89 (2019).

45. Fallahzadeh, R., Aref, L., Avargani, V. M., Gholamiarjenaki, N., An experimental investigation on the performance of a new portable active bubble basin solar still, *Appl. Therm. Eng.*, *181:* 115918 (2020).

46. Parikh, R., Patdiwala, U., Parikh, S., Panchal, H., Sadasivuni, K. K., Performance enhancement using TiO2 nano particles in solar still at variable water depth, *Int. J. Ambient Energy*, *43*(1): 4037-4044 (2022).

47. Shoeibi, S., Kargarsharifabad, H., Rahbar, N., Effects of nano-enhanced phase change material and nano-coated on the performance of solar stills, J. Energy Storage, 42: 103061 (2021).

48. Abdullah, A. S., Omara, Z. M., Essa, F. A., Younes, M. M., Shanmugan, S., Abdelgaied, M., ... Farouk, W. M., Improving the performance of trays solar still using wick corrugated absorber, nano-enhanced phase change material and photovoltaics-powered heaters, *J. Energy Storage*, *40:* 102782 (2021).

49. Kumar, P. M., Chauhan, P., Sharma, A. K., Rinawa, M. L., Rahul, A. J., Srinivas, M., Tamilarasan, A., Performance study on solar still using nano disbanded phase change material (NDPCM), Mater. Today: Proc. 62: 1894-1897 (2022).

50. Abdullah, A. S., Omara, Z. M., Essa, F. A., Alqsair, U. F., Aljaghtham, M., Mansir, I. B., ... Alawee, W. H., Enhancing trays solar still performance using wick finned absorber, nano-enhanced PCM, Alex. Eng. J., 61(12): 12417-12430 (2022).

51. Sathyamurthy, R. (2023)., Silver (Ag) based nanoparticles in paraffin wax as thermal energy storage for stepped solar still–An experimental approach, Sol Energy, 262: 111808.

52. Kandeal, A. W., El-Shafai, N. M., Abdo, M. R., Thakur, A. K., El-Mehasseb, I. M., Maher, I., ... Sharshir, S. W., Improved thermo-economic performance of solar desalination via copper chips, nanofluid, and nano-based phase change material, Sol. Energy, 224: 1313-1325 (2021).

53. Tuly, S. S., Ayon, A. B. S., Hassan, R., Das, B. K., Khan, R. H., Sarker, M. R. I., Performance investigation of active double slope solar stills incorporating internal sidewall reflector, hollow circular fins, and nanoparticle-mixed phase change material, J. Energy Storage, 55: 105660 (2022).

54. Ghandourah, E. I., Sangeetha, A., Shanmugan, S., Zayed, M. E., Moustafa, E. B., Tounsi, A., Elsheikh, A. H., Performance assessment of a novel solar distiller with a double slope basin covered by coated wick with lanthanum cobalt oxide nanoparticles, Case Stud. Therm. Eng., 32: 101859 (2022).

55. Yuvaraj, M., Sudharani, R., Suresh, R., Kumar, A., Raghuram, K. S., Influence of nano-coating on the productivity of a double slope solar still. Mater. Today: Proc., 69: 744-748 (2022).

56. Alqsair, U. F., Abdullah, A. S., Omara, Z. M., Enhancement the productivity of drum solar still utilizing parabolic solar concentrator, phase change material and nanoparticles' coating, J. Energy Storage, 55: 105477 (2022).

57. El Mir, L., Amlouk, A., Elaloui, E., Saadoun, M., Pierre, A. C., Preparation and optical characterization of transparent, microporous TiO2 xerogel monoliths, *Mater. Sci. Eng.: B*, *146*(1-3): 69-73 (2008).

58. Amor, C. O., Virlan, C., Pui, A., Elaloui, E., Effect of dysprosium ion (Dy3+) doping on morphological, crystal growth and optical properties of TiO2 particles and thin films, Phys. B: Condens. Matter, *560:* 67-74 (2019).

59. Dhaou, M., Elaloui, E., Khirouni, K., Guermazi, H., Guermazi, S., Enhancement of dielectric responses and conduction properties of Zn-doped TiO2 for energy storage and photosensitivity applications. *J Mater Sci Mater Electron*, *32*(10): 13187-13204 (2021).

60. Nichols, E. L., The luminescence of titanium oxide. Phys. Rev. *22*(5): 420 (1923).

61. Kachbouri, S., Elaloui, E., Moussaoui, Y., the effect of surfactant chain length and type on the photocatalytic activity of mesoporous TiO2 nanoparticles obtained via modified sol-gel process, *Iran. J. Chem. Chem. Eng.*, *38*(1): 17-26 (2019).

62. Jraba, A., Anna, Z., Elaloui, E., Effects of Sr2+, Fe3+ and Al3+ doping on the properties of TiO2 prepared using the sol–gel method, *C R Chim*, *22*(9-10): 648-658 (2019).

63. Abdelgaied, M., Attia, M. E. H., Kabeel, A. E., Zayed, M. E., Improving the thermo-economic performance of hemispherical solar distiller using copper oxide nanofluids and phase change materials: Experimental and theoretical investigation, *Sol. Energy Mater Sol. Cells*, *238:* 111596 (2022).

64. Kabeel, A. E., Attia, M. E. H., Zayed, M. E., Abdelgaied, M., Abdullah, A. S., El-Maghlany, W. M., Performance enhancement of a v-corrugated basin hemispherical solar distiller combined with reversed solar collector: An experimental approach, Renew. Energy, 190: 330-337 (2022).

65. Beggas, A., Abdelgaied, M., Attia, M. E. H., Abdulla, A. S., Abdel-Aziz, M. M., Improving the freshwater productivity of hemispherical solar distillers using waste aluminum as store materials, *J. Energy Storage*, *60:* 106692 (2023).

66. Attia, M. E. H., Zayed, M. E., Kabeel, A. E., Abdullah, A. S., Abdelgaied, M., Energy, exergy, and economic analyses of a modified hemispherical solar distiller augmented with convex absorber basin, wicks, and PCM, *Sol. Energy*, *261*: 43-54 (2023).

67. Sathyamurthy, R., El-Maghlany, W. M., Attia, M. E. H., Kabeel, A. E., Abdelgaied, M., M. Abdel-Aziz, M., ... Vasanthaseelan, S., Hemispherical Solar Distiller Performance Utilizing Hybrid Storage Media, Paraffin Wax with Nanoparticles: An Experimental Study. *Molecules*, *27*(24): 8988 (2022).

68. Vaithilingam, S., Muthu, V., Athikesavan, M. M., Afzal, A., Sathyamurthy, R., Energy and exergy analysis of conventional acrylic solar still with and without copper fins, *Environ. Sci. Pollut. Res.*, 1-11 (2021).

69. Muthu Manokar, A., Vimala, M., Prince Winston, D., Rajendran, D. R., Sathyamurthy, R., & Kabeel, A. E., A comparative study of 3E (energy, exergy, and economy) analysis of various solar stills, *Heat Transfer.*, *49*(8) : 4394-4409 (2020).

70. Muthu Manokar, A., Vimala, M., Prince Winston, D., Rajendran, D. R., Sathyamurthy, R., & Kabeel, A. E., Year around distilled water production, energy, and economic analysis of solar stills—a comparative study, *Heat Transfer*, *49*(6) : 3651-3662 (2020).

71. Tei E.A., Hameed R.M.S., Illyas M., Athikesavan M.M., Experimental investigation of inclined solar still with and without sand as energy storage materials, J. Energy Storage, 77, Article 109809 (2024).